USGS
science for a changing world

Emplacement of Holocene Silicic Lava Flows and Domes at Newberry, South Sister, and Medicine Lake Volcanoes, California and Oregon

Scientific Investigations Report 2017–5022–I

U.S. Department of the Interior
U.S. Geological Survey

Cover: Photograph showing folded crease structure in coarsely vesicular pumice on northwest lobe of Little Glass Mountain rhyolite flow, Medicine Lake Volcano, California.

Emplacement of Holocene Silicic Lava Flows and Domes at Newberry, South Sister, and Medicine Lake Volcanoes, California and Oregon

By Jonathan H. Fink and Steven W. Anderson

Scientific Investigations Report 2017–5022–I

U.S. Department of the Interior
U.S. Geological Survey

U.S. Department of the Interior
RYAN K. ZINKE, Secretary

U.S. Geological Survey
William H. Werkheiser, Acting Director

U.S. Geological Survey, Reston, Virginia: 2017

Suggested citation:
Fink, J.H., and Anderson, S.W., 2017, Emplacement of Holocene silicic lava flows and domes at Newberry, South Sister, and Medicine Lake volcanoes, California and Oregon: U.S. Geological Survey Scientific Investigations Report 2017–5022–I, 41 p., https://doi.org/10.3133/sir20175022I.

ISSN 2328-0328 (online)

Preface

The North American Cordillera is home to a greater diversity of volcanic provinces than any comparably sized region in the world. The interplay between changing plate-margin interactions, tectonic complexity, intra-crustal magma differentiation, and mantle melting have resulted in a wealth of volcanic landscapes. Field trips in this series visit many of these landscapes, including (1) active subduction-related arc volcanoes in the Cascade Range; (2) flood basalts of the Columbia Plateau; (3) bimodal volcanism of the Snake River Plain-Yellowstone volcanic system; (4) some of the world's largest known ignimbrites from southern Utah, central Colorado, and northern Nevada; (5) extension-related volcanism in the Rio Grande Rift and Basin and Range Province; and (6) the spectacular eastern Sierra Nevada featuring Long Valley Caldera and the iconic Bishop Tuff. Some of the field trips focus on volcanic eruptive and emplacement processes, calling attention to the fact that the western United States provides opportunities to examine a wide range of volcanological phenomena at many scales.

The 2017 Scientific Assembly of the International Association of Volcanology and Chemistry of the Earth's Interior (IAVCEI) in Portland, Oregon, marks the first time that the U.S. volcanological community has hosted this quadrennial meeting since 1989, when it was held in Santa Fe, New Mexico. The 1989 field-trip guides are still widely used by students and professionals alike. This new set of field guides is similarly a legacy collection that summarizes decades of advances in our understanding of magmatic and tectonic processes of volcanic western North America.

The field of volcanology has flourished since the 1989 IAVCEI meeting, and it has profited from detailed field investigations coupled with emerging new analytical methods. Mapping has been enhanced by plentiful major- and trace-element whole-rock and mineral data, technical advances in radiometric dating and collection of isotopic data, GPS (Global Positioning System) advances, and the availability of lidar (light detection and ranging) imagery. Spectacularly effective microbeam instruments, geodetic and geophysical data collection and processing, paleomagnetic determinations, and modeling capabilities have combined with mapping to provide new information and insights over the past 30 years. The collective works of the international community have made it possible to prepare wholly new guides to areas across the western United States. These comprehensive field guides are available, in large part, because of enormous contributions from many experienced geologists who have devoted entire careers to their field areas. Early career scientists are carrying forward and refining their foundational work with impressive results.

Our hope is that future generations of scientists as well as the general public will use these field guides as introductions to these fascinating areas and will be enticed toward further exploration and field-based research.

Michael Dungan, University of Oregon
Judy Fierstein, U.S. Geological Survey
Cynthia Gardner, U.S. Geological Survey
Dennis Geist, National Science Foundation
Anita Grunder, Oregon State University
John Wolff, Washington State University

Field-trip committee, IAVCEI 2017

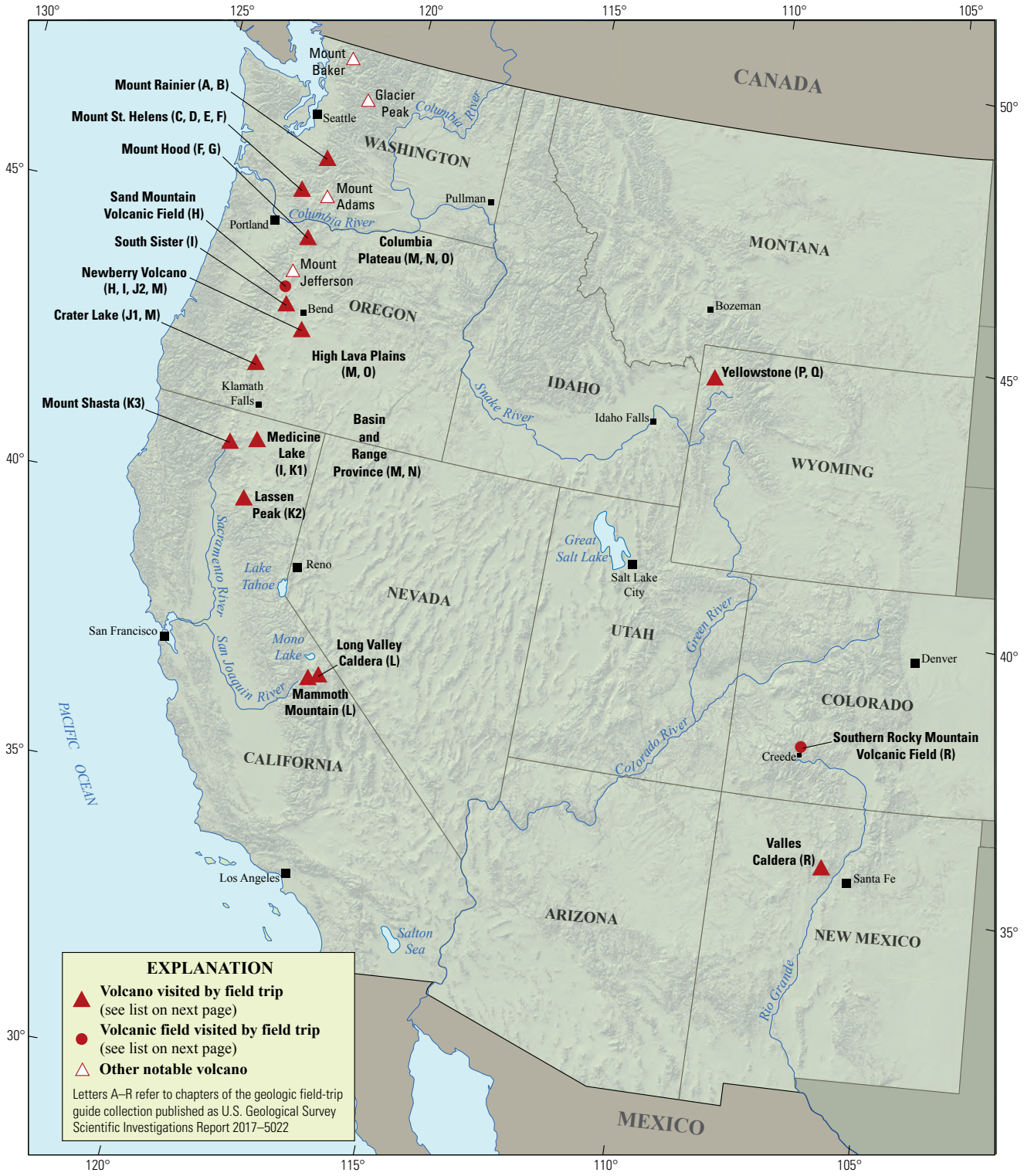

Map of the western United States showing volcanoes and volcanic fields visited by geologic field trips scheduled in conjunction with the 2017 meeting of the International Association of Volcanology and Chemistry of the Earth's Interior (IAVCEI) in Portland, Oregon, and available as chapters in U.S. Geological Survey Scientific Investigations Report 2017–5022. Shaded-relief base from U.S. Geological Survey National Elevation Dataset 30-meter digital elevation model data.

Contributing Authors

Boise State University
Brittany D. Brand
Nicholas Pollock

Colgate University
Karen Harpp
Alison Koleszar

Durham University
Richard J. Brown

Eastern Oregon University
Mark L. Ferns

ETH Zurich
Olivier Bachmann

Georgia Institute of Technology
Josef Dufek

GNS Science, New Zealand
Natalia I. Deligne

Hamilton College
Richard M. Conrey

Massachusetts Institute of Technology
Timothy Grove

National Science Foundation
Dennis Geist (also with Colgate University and University of Idaho)

New Mexico Bureau of Geology and Mineral Resources
Paul W. Bauer
William C. McIntosh
Matthew J. Zimmerer

New Mexico State University
Emily R. Johnson

Northeastern University
Martin E. Ross

Oregon Department of Geology and Mineral Industries
William J. Burns
Lina Ma
Ian P. Madin
Jason D. McClaughry

Oregon State University
Adam J.R. Kent

Portland State University
Jonathan H. Fink (also with University of British Columbia)
Martin J. Streck
Ashley R. Streig

San Diego State University
Victor E. Camp

Smithsonian Institution
Lee Siebert

Universidad Nacional Autónoma de San Luis Potosi
Damiano Sarocchi

University of California, Davis
Kari M. Cooper

University of Liverpool
Peter B. Kokelaar

University of Northern Colorado
Steven W. Anderson

University of Oregon
Ilya N. Binderman
Michael A. Dungan
Daniele Mckay (also with Oregon State University and Oregon State University, Cascades)

University of Portland
Kristin Sweeney

University of Tasmania
Martin Jutzeler
Jocelyn McPhie

University of Utah
Jamie Farrell

U.S. Army Corps of Engineers
Keith I. Kelson

U.S. Forest Service
Gordon E. Grant (also with Oregon State University)

U.S. Geological Survey
Charles R. Bacon
Andrew T. Calvert
Christine F. Chan
Robert L. Christiansen
Michael A. Clynne
Michael A. Cosca
Julie M. Donnelly-Nolan
Benjamin J. Drenth
William C. Evans
Judy Fierstein
Cynthia A. Gardner
V.J.S. Grauch
Christopher J. Harpel
Wes Hildreth
Richard P. Hoblitt
Robert A. Jensen
Peter W. Lipman
Jacob B. Lowenstern
Jon J. Major
Seth C. Moran
Lisa A. Morgan
Leah E. Morgan
L.J. Patrick Muffler
Jim O'Connor
John S. Pallister
Thomas C. Pierson
Joel E. Robinson
Juliet Ryan-Davis
Kevin M. Scott
William E. Scott
Wayne (Pat) Shanks
David R. Sherrod
Thomas W. Sisson
Mark Evan Stelten
Weston Thelen
Ren A. Thompson
Kenzie J. Turner
James W. Vallance
Alexa R. Van Eaton
Jorge A. Vazquez
Richard B. Waitt
Heather M. Wright

U.S. Nuclear Regulatory Commission
Stephen Self (also with University of California, Berkeley)

Washington State University
Joseph R. Boro
Owen K. Neill
Stephen P. Reidel
John A. Wolff

Acknowledgments
Juliet Ryan-Davis and Kate Sullivan created the overview map, and Vivian Nguyen created the cover design for this collection of field-trip guide books. The field trip committee is grateful for their contributions.

Contents

Figures

Emplacement of Holocene Silicic Lava Flows and Domes at Newberry, South Sister, and Medicine Lake Volcanoes, California and Oregon

By Jonathan H. Fink[1] and Steven W. Anderson[2]

Introduction

This field guide for the International Association of Volcanology and Chemistry of the Earth's Interior (IAVCEI) Scientific Assembly 2017 focuses on Holocene glassy silicic lava flows and domes on three volcanoes in the Cascade Range in Oregon and California: Newberry, South Sister, and Medicine Lake volcanoes. Although obsidian-rich lava flows have been of interest to geologists, archaeologists, pumice miners, and rock hounds for more than a century, many of their emplacement characteristics had not been scientifically observed until two very recent eruptions in Chile. Even with the new observations, several eruptive processes discussed in this field trip guide can only be inferred from their final products. This makes for lively debates at outcrops, just as there have been in the literature for the past 30 years.

Of the three volcanoes discussed in this field guide, one (South Sister) lies along the main axis defined by major peaks of the Cascade Range, whereas the other two lie in extensional tectonic settings east of the axis (fig. 1). These two tectonic environments influence volcano morphology and the magmatic and volcanic processes that form silicic lava flows and domes. The geomorphic and textural features of glass-rich extrusions provide many clues about their emplacement and the magma bodies that fed them.

The scope of this field guide does not include a full geologic history or comprehensive explanation of hazards associated with a particular volcano or volcanic field. The geochemistry, petrology, tectonics, and eruption history of Newberry, South Sister, and Medicine Lake volcanic centers have been extensively studied and are discussed on other field excursions. Instead, we seek to explore the structural, textural, and geochemical evolution of well-preserved individual lava flows—the goal is to understand the geologic processes, rather than the development, of a specific volcano.

Glassy lava flows are a subset of silicic extrusions. Steeper sided, more crystal rich andesite, dacite, and rhyodacite lava domes have been scientifically observed and measured while active in, or near the summit craters of, many composite volcanoes since the start of the 20th century. These crystal-rich eruptions occurred at Montagne Pelée (Martinique, 1902–07; Roobol and Smith, 1975), Santa Maria (Guatemala, 1922–present; Rose, 1987), La Soufrière (St. Vincent, 1979; Huppert and others, 1982), Mount St. Helens (Washington, USA, 1980–86; Swanson and Holcomb, 1990), Mount Unzen (Japan, 1991–95; Nakada and others, 1999), and Soufrière Hills (Montserrat, 1995–present; Watts and others, 2002). Many publications describing these eruptions (including those referenced above) focus on physical process questions, like we will do in this field guide.

In contrast with the silicic extrusions found near summit craters, the glassy lava flows we will visit are commonly found on the flanks of volcanoes. The flows are exposed in extensive glassy outcrops intermixed with a variety of pumiceous textures on the surfaces and in flow fronts, are mostly thinner and flatter, and are commonly found in aligned groups inferred to have been fed by dikes.

Although eruption styles can vary, dome-forming eruptions commonly include one or more Plinian explosive phases, followed by quieter emplacement of silicic lavas through vents near the summit. This transition has been attributed to either decreasing magma volatile content, slower magma ascent rates allowing more volatiles to escape into the country rock, or a combination of the two. In some eruptions, the fronts of quietly effusing domes can collapse explosively, generating deadly pyroclastic flows. Understanding why eruptive styles transition from explosive to effusive and back to explosive is one of the primary motivations for studying silicic flows and domes.

Volatile contents preserved in lava extrusions reflect a combination of pre-, syn-, and post-eruptive processes. This field trip will examine the variability and two- and three-dimensional distribution of vesicular and glassy textures found on silicic lava flow surfaces, fronts, and (when exposed by erosion or drill cores) interiors. Distinguishing between meteoric and magmatic water contents and correlating the latter with textures can provide further insights into eruptive processes.

In this field guide, we will reference models used to explain several of the structural and textural features observed

[1]Portland State University.

[2]University of Northern Colorado.

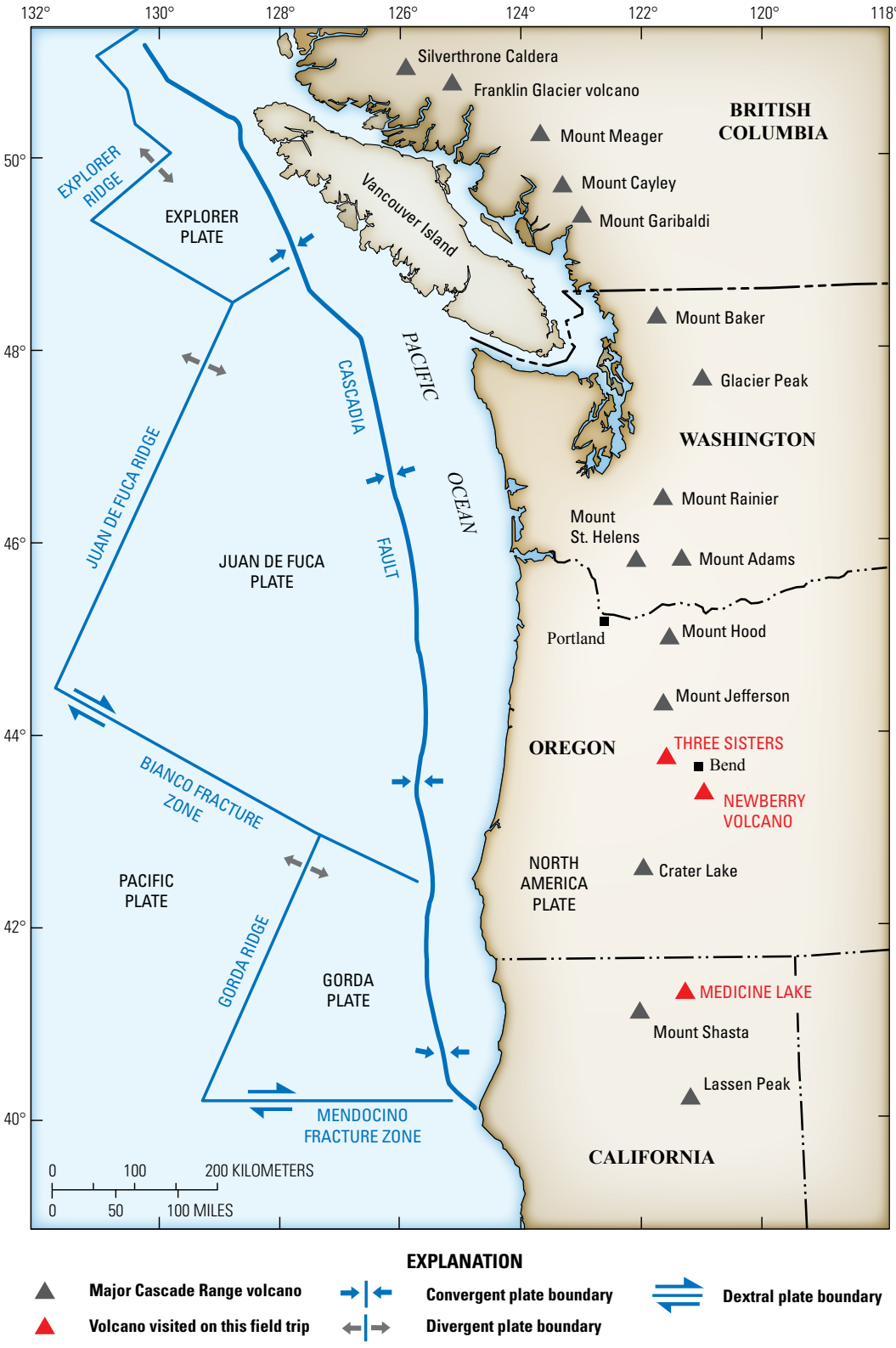

Figure 1. Map showing major Cascade volcanoes along primary volcanic arc and geometry of subducting oceanic plates to the west. Note that Medicine Lake and Newberry volcanoes are located east of the trend of major Cascade volcanoes. Map modified from National Aeronautics and Space Administration (NASA).

at one or more stops; we will discuss these concepts in more detail during the field trip. The phenomena and processes to be discussed include distribution of block sizes on flow surfaces; transverse surface folds formed by flow-parallel compression; smooth-sided, outwardly convex "crease structure" fractures that tend to orient parallel to flow direction; diapirs of coarsely vesicular pumice punctuating the flow surface that sometimes display regular spacing in the downflow direction; discrete and gradational contacts among different pumiceous and glassy textures, including prominent spines of finely vesicular pumice that grade downward into obsidian; circular explosion craters as much as 5 meters (m) deep sourced in volatile-rich zones of the flow interior; post-emplacement rehydration of the flow surface by precipitation; subparallel pairs of ground cracks and pits in surrounding areas that mark positions and orientations of subsurface feeder dikes; and morphologic progressions among adjacent domes that reflect tradeoffs between effusion and cooling rates based on comparisons with laboratory simulations.

We have already mentioned that some of the features we will see in the field have never been observed in formation, because active rhyolitic obsidian lava flows have never been scientifically witnessed. However, emplacement of a large rhyodacite lava flow and a rhyolitic summit dome were observed in Chile in the past decade. The 2011–13 eruption of Puyehue-Cordón Caulle in central Chile produced an extensive rhyodacite flow revealing several structural processes and products (but not the full range of textural variations) that had previously only been inferred from flows like the ones we will visit on this field trip. This eruption also provided new insights into how quickly large glassy flows can advance, and how long lava effusion can be accompanied by ongoing explosive ash emissions. The glass-rich rhyolite dome produced by the 2008–09 eruption of Chaitén volcano in Chile resembled many of the earlier cited, crystal-rich domes of less silicic composition. Neither of these eruptions generated all of the textural and structural characteristics that are the hallmarks of the flows we will visit; however, in this field guide, we reference a few recent observations of the Cordón Caulle flow and the Chaitén dome.

Road Log

Numbers at left are distances in miles from starting point. Numbers in bold at the end of each entry are the distance in miles to the next entry. An overview of field trip stops and major routes is shown in figure 2. A detailed map of road names in the Modoc National Forest can be accessed at https://www.fs.usda.gov/detailfull/modoc/maps-pubs/?cid=FSEPRD533310&width=full.

Day 1—Portland to Bend, Oregon, With a Stop at Newberry Volcano

0.0 From the Oregon Convention Center in Portland, travel east on Interstate 84 and U.S. Highway No. 26 (U.S. 26) through Government Camp on the south flank of Mount Hood. (Weather permitting, we may take a 5.5-mile detour just south of Government Camp along Timberline Road to the parking lot for Timberline Lodge to get closer views of Mount Hood and the Cascade Range volcanoes to the south. This stop is not reflected in the road log.) Continue south on U.S. 26, passing through the Warm Springs Reservation, to the junction of U.S. Highway No. 97 (U.S. 97) in Madras. Turn right onto U.S. 97 to continue to Bend, Oregon. The first part of the route passes by several Pliocene-Pleistocene Boring volcanic rocks and volcanoes, which dot metropolitan Portland. Portland is the only mid-to large-sized city in the continental United States that contains many young (less than 300,000 years old) volcanic centers. On clear days, this route has several good views of Mount Hood, Oregon's tallest mountain and volcano at 11,249 feet (ft) (3,429 m). Mount Hood has had three eruptive episodes in the past 1,800 years, mostly producing lava domes that collapsed to generate pyroclastic flows and lahars (Gardner and others, 2000). **118.0**

118.0 Turn right at junction of U.S. 26 and U.S. 97 in Madras, Oregon. The drive from Madras to Bend offers excellent views of several Cascade volcanoes, including Mount Jefferson (10,497 ft; 3,199 m), Mount Washington (7,798 ft; 2,377 m), North Sister (10,085 ft; 3,074 m), Middle Sister (10,047 ft; 3,062 m) and South Sister (10,358 ft; 3,157 m). **40.0**

158.0 Junction of U.S. Highway No. 20 and U.S. 97 (Bend, Oregon). Continue heading south on U.S. 97. High-alumina olivine basalts are visible in outcrops for the next 18 kilometers (km). These flows comprise the lower slopes of Newberry Volcano (fig. 3), the most voluminous and one of the most areally extensive of the Cascade volcanoes, at more than 1,300 square kilometers (km^2) (Donnelly-Nolan and others, 2011a). Newberry lies 30 km east of the main Cascade axis. **10.0**

168.0 Outcrops of exposed cinder cone dated at about 7,000 years before present (7 ka) (Donnelly-Nolan and others, 2011a). **13.3**

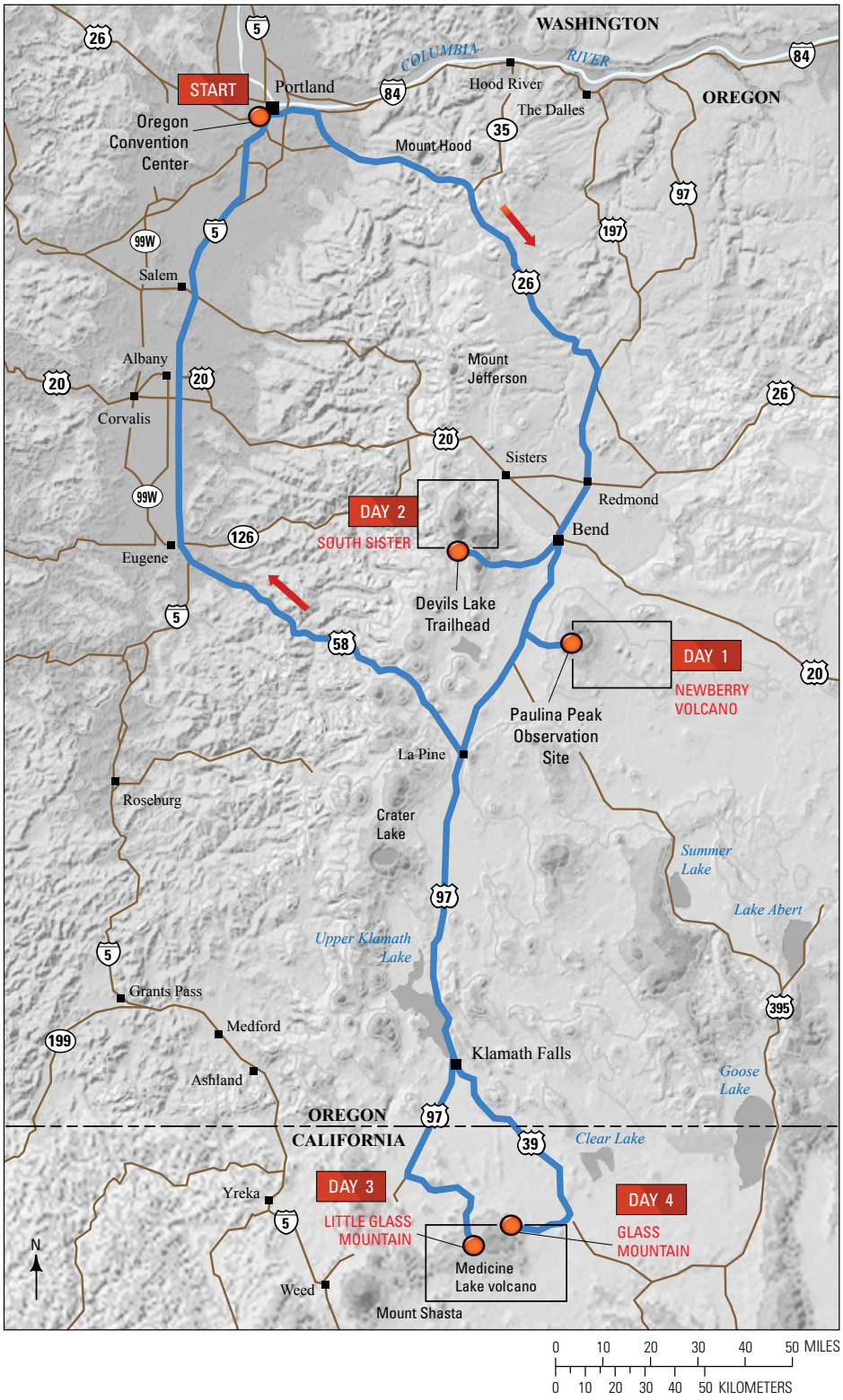

Figure 2. Map showing overview of field trip route (blue lines). Day 1, Portland, Oregon, to Newberry Volcano; Day 2, Bend, Oregon, to South Sister volcano; Day 3, Bend, Oregon, to Little Glass Mountain and west side Medicine Lake volcano; Day 4, Tulelake, California, to Glass Mountain and east side of Medicine Lake volcano. Nights 1 and 2 near Bend, Oregon. Night 3 near Tulelake, California. Red arrows show general direction of field trip route.

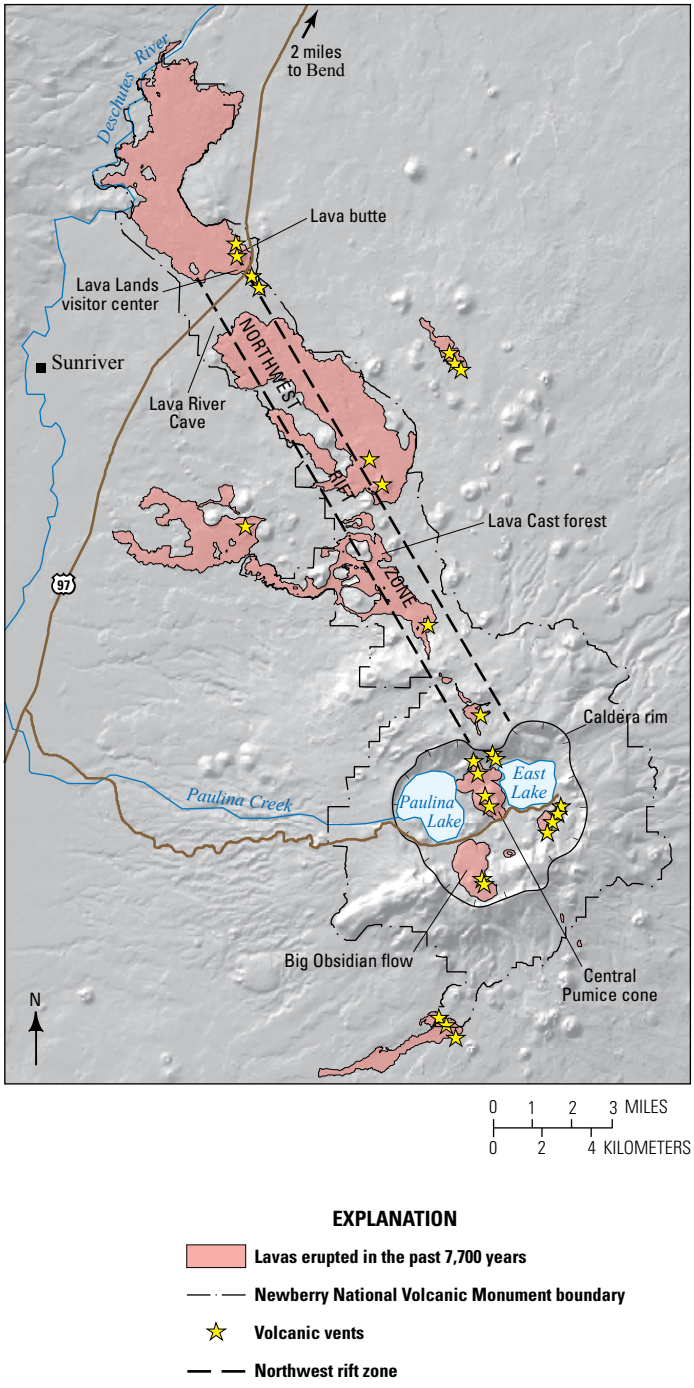

Figure 3. Map showing structure of Newberry Volcano and prominent northwest-trending fracture zone that extends from Lava Butte near Bend to Newberry caldera (Donnelly-Nolan and others, 2011a).

181.3 Turn left (east) onto Paulina Lake Road (U.S. Forest Service Road 21 [NF 21]). **12.8**

194.1 Turn right (south) onto U.S. Forest Service Road 500 (NF 500). **3.9**

198.0 **Stop 1. Paulina Peak (elevation 7,984 ft; 2,434 m) 3.9**

This stop provides an overview of Holocene Newberry Volcano, its recent silicic lavas, and the main Cascade volcanoes to the west (fig. 4). Walk north to view the 7- to 8-km-wide caldera that formed during multiple Holocene pyroclastic events (MacLeod and others, 1981; Donnelly-Nolan, 2011a). Paulina Lake and East Lake define the extent of the caldera, whereas the prominent Big Obsidian Flow (~1.3 ka, ~72 percent SiO_2, and probably the most recent eruption of Newberry; MacLeod and others, 1981; Donnelly-Nolan, 2011a) flowed north from the southern caldera boundary. Several other silicic flows can be seen from this stop, including the Inter Lake Flow and the East Lake obsidian flows (~3.5 ka), all of which appear to have emerged from fractures along the caldera margins. Mount Bachelor, and South, Middle, and North Sister volcanoes are visible to the northwest along the main axis of the Cascade Range. The morphology and lava flow distribution of off-axis Newberry Volcano contrast with those of the on-axis South Sister volcano (Day 2 field stops).

Big Obsidian Flow formed during and after pyroclastic flow and fall emplacement that is evident to the east of the vent. Structures and textures in the flow are common to many rhyolitic obsidian flows. The flow has an elevated vent area containing deep fractures and large blocks that grade outward to an area of prominent flow ridges composed of smaller blocks. Anderson and others (1998) found that block sizes in active flow and dome vent areas correlate inversely with extrusion rates: large blocks form in low extrusion rate conditions whereas smaller blocks result from higher extrusion rates. Large blocks in the Big Obsidian Flow vent result from low extrusion rates that characteristically mark the final stages of an eruption. Blocks created in vent areas are transported down flow where they break into smaller blocks, resulting in smaller average block sizes downslope. Fink and Griffiths (1998) observed similar relations in laboratory simulations of lava domes using slurries of kaolin and polyethylene glycol wax.

Transverse ridges on silicic lava flows have been interpreted to be folds caused by flow-parallel compression (Fink, 1980a) analogous to the “ropes” on pāhoehoe basalt flows. These ridges sometimes expose in the fold crests new, larger blocks from the flow interior, whereas small blocks accumulate in the

Figure 4. Image of Newberry Volcano caldera, showing Big Obsidian Flow, East Lake obsidian flow, and Inter Lake Flow which entered Paulina Lake and East Lake.

fold troughs and sift beneath the flow surface through the gaps between larger blocks, resulting in an average block size that remains relatively constant in the folded parts of the flow surface.

Big Obsidian Flow (fig. 5) displays a characteristic suite of three textural end members recognized at many other rhyolitic obsidian flows. The lightest shades of surface blocks exhibit a nearly aphyric finely vesicular pumice (FVP) texture (Fink, 1980b, 1983; Fink and Manley, 1987) of submillimeter-sized vesicles that are typically difficult to discern without the use of a hand lens. Darker areas consist of relatively thin bands of dense obsidian (OBS) that separate the FVP from a coarsely vesicular pumice unit (CVP), which displays macroscopic bubbles that may approach one centimeter in diameter.

These three textures are commonly found in lava flow fronts in a consistent stratigraphy of a 5- to 10-m-thick layer of FVP on top, underlain by 1- to 5-m-thick layer of OBS, and a layer of CVP that extends downward from the OBS until flow front talus obscures the lower parts of the flow. Research drilling at Obsidian Dome in California and the

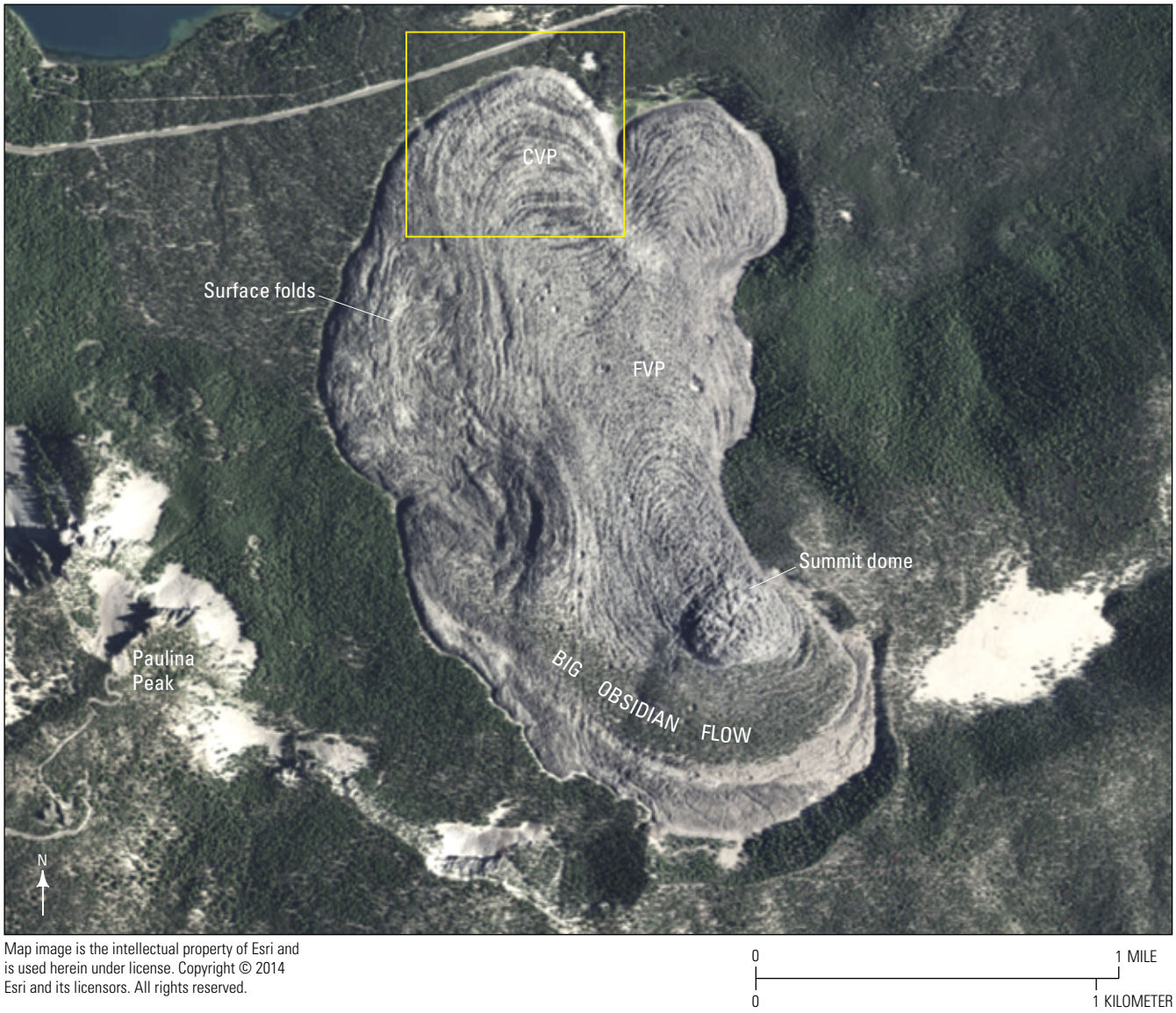

Figure 5. Image showing Big Obsidian Flow and prominent compressional ridges near northernmost flow front and circular dome (summit dome) over vent area. Yellow box shows location of figure 8. Abbreviations: CVP, coarsely vesicular pumice; FVP, finely vesicular pumice.

Banco Bonito flow in New Mexico revealed a more complete internal stratigraphy (fig. 6) consisting of FVP at the surface, underlain by OBS, CVP, and another layer of OBS, a central partly crystallized rhyolite core, a lower OBS, and a basal breccia.

Fink and Manley (1987) and Manley and Fink (1987) proposed an emplacement model of texture formation beginning with the extrusion of dense obsidian, the upper surface of which vesiculates because of low pressure, creating FVP. The central part of the flow remains hot long enough to allow crystallization to occur during flow advance, forming the central rhyolite core, which grades upward and downward into the original obsidian. Crystallization of the central rhyolite releases water vapor, which migrates upward through the OBS by way of microcracks formed by shear stresses transmitted from the base of the advancing lava flow. This microfracturing is unable to reach the uppermost part of the flow, resulting in an unfractured level in the OBS, below which the rising volatiles accumulate.

Bubbles grow slowly in the volatile-enriched zone, leading to formation of the coarsely vesicular pumice (CVP) texture. The relatively high water content and low

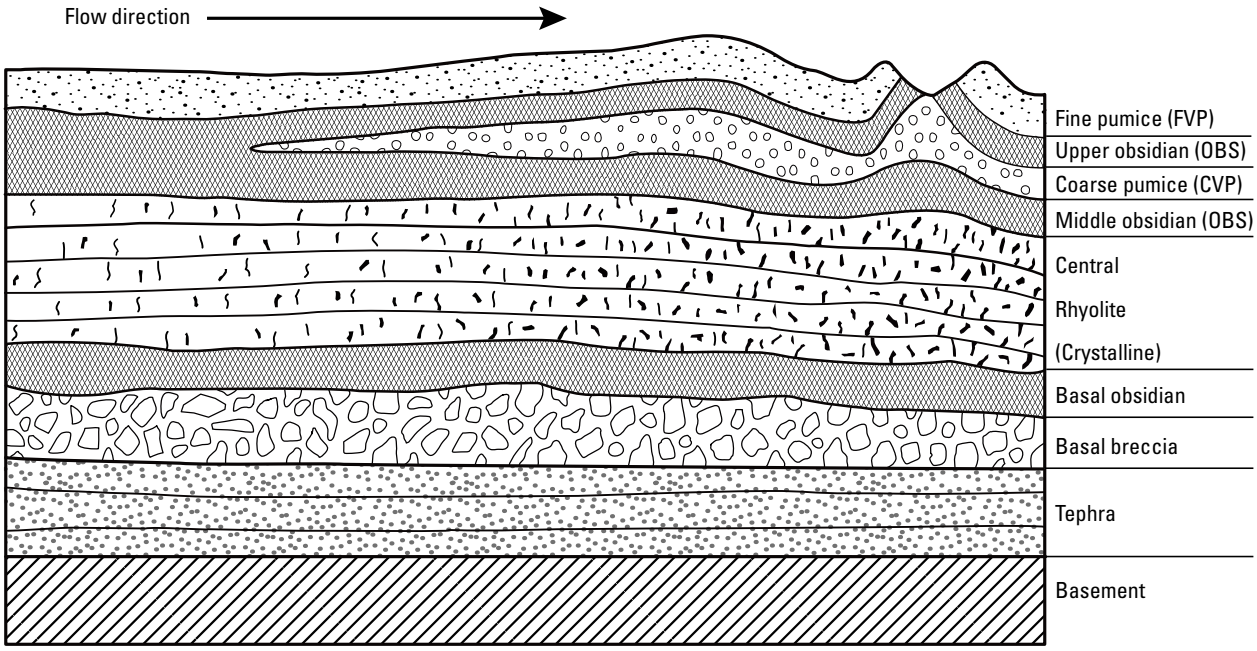

Figure 6. Schematic cross section of a rhyolitic obsidian flow based on drill core observations from Obsidian Dome in the Inyo dome chain, eastern California. Only the top two or three layers are typically exposed in a flow front. This interpretation assumes that a flow is emplaced initially as obsidian, the top of which effervesces to form finely vesicular pumice (FVP), while the interior crystallizes, and accumulating volatiles form the coarsely vesicular pumice (CVP). This interpretation contrasts with the "permeable foam" model of Eichelberger and others (1986), which assumes the entire flow starts as froth that compresses in places to form obsidian. Figure from Fink and Manley (1987).

density of the volatile-enriched layer allow it to rise to the flow surface as dark, regularly spaced diapirs, which can be stretched and folded as the flow lobes that contain them advance. In certain conditions, this water-rich zone can also generate local explosions that blast through to the flow surface and produce explosion craters.

From Paulina Peak, it is possible to see some of these features on Big Obsidian Flow. Dark outcrops of CVP make up much of the distal flow margin, particularly the westernmost part. Surface folds are prominent. A few explosion craters are visible about midway between the summit dome and the flow front.

Eichelberger and others (1986) proposed an alternative emplacement model in which rhyolitic extrusions are composed of permeable magmatic foam that collapses into obsidian as it rises through the upper parts of the conduit and then flows away from the vent. The FVP represents the uncollapsed foam that did not have sufficient overburden to compress the fine bubbles. The CVP and other lower units revealed during research drilling were not accounted for in the Eichelberger and others model.

These competing models originated without observation of active rhyolitic obsidian flows. Little was known about glassy rhyolite lava emplacement until 2008 when a multilobed rhyolitic obsidian dome was erupted at Chaitén volcano in Chile (Pallister and others, 2013). This eruption produced a small, spiny extrusion (less than 1 km in total length) that has little morphological similarity to flows at Newberry, South Sister, and Medicine Lake volcanoes. However, in 2011, an eruption at the Cordón Caulle volcano in Chile produced a large, dike-fed rhyodacitic obsidian flow that was observed remotely and in the field (fig. 7; Tuffen and others, 2013). The Cordón Caulle flow has many morphological similarities to the extrusions we will see on this field trip, including folds, textural contrasts, and crease structures (Anderson and Fink, 1992); however, this flow lacks the full textural spectrum seen in glassy rhyolite flows in Oregon and California.

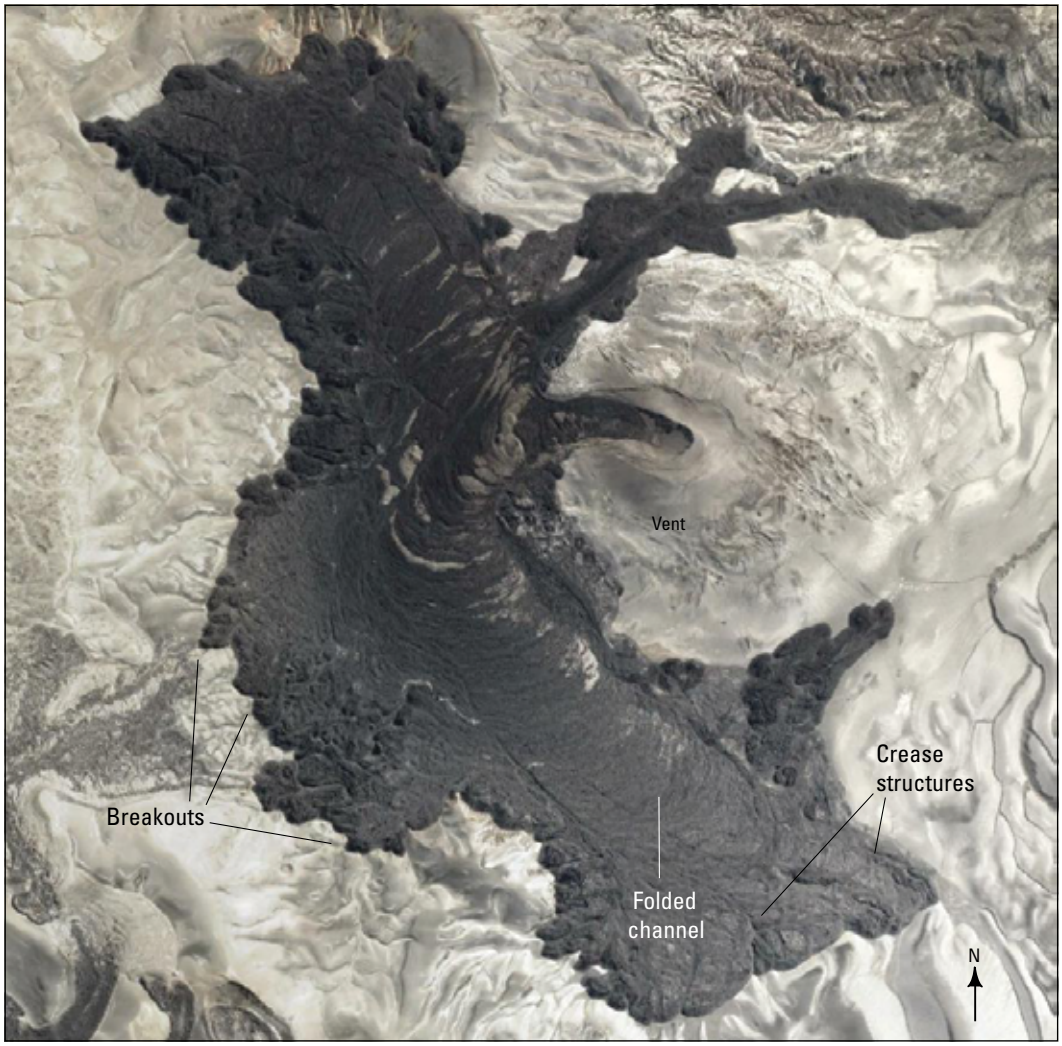

Figure 7. Google Earth image of the 2011–13 Cordón Caulle rhyodacite lava flow (CC) in Chile. CC has some structural similarities to the domes we will visit on this trip, especially the flow-parallel crease structures. However, CC flow margins are more scalloped, reflecting marginal breakouts, and the upper surface is more texturally uniform, similar to morphology of the earliest emplaced dacite lobe at Glass Mountain on Medicine Lake volcano (see fig. 43). Large, light-colored areas near central part of flow are rafted pieces of the cone through which initial pyroclastic flows erupted.

Several observations of the Cordón Caulle flow may help constrain interpretations of prehistoric extrusions like the ones we will visit. First, the Cordón Caulle flow inflated significantly during emplacement, similar to observed Hawaiian basalt flows (Hon and others, 1994). Inflation of the Chilean flow appears to have occurred when stagnating flow fronts prevented erupted magma from advancing, increasing flow thickness. As the flow matured, several breakouts emanated from the stagnant margins some months after extrusion ceased in the vent area, suggesting the flow interior was sufficiently thermally insulated to remain mobile long after effusion stopped (Anderson and others, 2005). There was no evidence of flow recompression after eruption ceased (Castro and others, 2013; Farquharson and others, 2015).

A second observation germane to the formation of silicic lava textures is that 2011–13 Cordón Caulle flow emplacement was accompanied by significant explosive jetting of pyroclastic material. These findings, combined with hydrogen isotope data, led to a revised model for rhyolitic lava effusion that proposes significant amounts of volatiles are released in batches through intermittently open pyroclastic channels that form tuffisite when they get incorporated into the resulting lava flow. This process allows volatiles that exsolve within a closed system in the conduit to escape explosively at the vent, allowing more degassed material to emerge at the surface (Castro and others, 2013). If the remaining lava contains sufficient volatiles, an additional surface phase of degassing may occur, as observed at Mount St. Helens (Swanson and Holcomb, 1990; Anderson and Fink, 1989, 1990) and inferred at many of the recent rhyolitic flows in the western United States (Fink and Manley, 1987). We will see textural evidence of pyroclastic jetting at several of the Medicine Lake volcano flows.

Return to vans and retrace route to NF 21.

201.9 Turn right onto NF 21. **1.9**

203.8 Turn right into parking lot for Big Obsidian Flow trailhead. **0.1**

203.9 Stop 2. Big Obsidian Flow at Newberry Volcano

At this stop, we'll discuss silicic lava surface textures and structures, and what they tell us about lava flow emplacement processes. We will also revisit the different models for emplacement of silicic lava flows and discuss the use of new instrumentation for studying these challenging flows in the field.

The rhyolitic Big Obsidian Flow was emplaced about 1,300 years ago (Donnelly-Nolan, 2011b) and has a volume of 0.1 cubic kilometers (km^3) (Gardner and others, 1998). This volume is like some well-studied flows in the western United States (such as Obsidian Dome in California at 0.14 km^3) but is significantly smaller than the Cordón Caulle flow of 2011–13 (more than 0.5 km^3; Farquharson and others, 2015).

We will walk along the trail that climbs onto the flow from the parking lot, but frequently will go off path to observe blocks, textures, and structures. The front and upper surface of the flow reveal three main textures that we will encounter throughout the field trip: finely vesicular pumice (FVP) carapace, dense obsidian (OBS), and coarsely vesicular pumice (CVP) (figs. 8 and 9). The trail also crosses structures that result from a combination of processes that we began discussing on Paulina Peak and will continue to see throughout the trip.

Flow Front: The first feature of note is the steep flow front. If lava flows were isothermal viscous fluids, they would thin out and pond as they spread, coming to rest with margins controlled only by pre-existing topography. However, the formation of temperature-dependent yield strength creates steep flow margins that can be tens of meters thick. Flow thickness depends on a balance between spreading rate and cooling rate; the faster a flow advances, the less opportunity it has to cool, and the thinner the resulting flow front. The "caterpillar-tread" movement of a blocky lava flow, through which blocks fall off the flow front and are overridden, commonly forms an apron of talus that resists forward flow motion, connecting with an underlying basal blocky layer. To get to the upper surface of the flow, the trail climbs up this prism of loose blocks, which conceals the lower half of the flow textural stratigraphy.

Surface folds: At first glance, the surface of an obsidian flow appears to be a chaotic mixture of blocks, spines, and hillocks of different colors, sizes, densities, crystallinity, and vesicularity. However, on aerial photos (or after one stumbles around for a few hours), patterns begin to emerge. Figures 5 and 8 show transverse flow ridges that form by compression of the upper flow surface. The spacing (wavelength) of the ridges (surface folds) is proportional to the thickness of the cooled flow crust. Because the flow crust generally thickens as a flow advances away from the vent, the wavelength increases. The amplitude (height) of the ridges also tends to increase with distance from the vent. Hence, the ridges are generally tallest near the flow front. Flow-parallel compression of an isothermal fluid would cause it to thicken—it is the rheology contrast between the surface and interior of a flow that results in selective amplification of certain wavelengths, and these ridges are what we observe snaking across the top of the flow, roughly parallel to the flow front. Flows are folded by compression that typically occurs where the slope beneath a flow decreases, causing lava to pile up and push against earlier emplaced material. From Paulina Peak, the start of flow folds is visible just downslope of the steep-sided conical vent area of the flow. When viewed from above, the sinuous trace of these flows outlines the irregular advance of the flow front.

Textural variations: The place where the trail emerges onto the upper flow surface is dominated by dark CVP lava that has been stretched during flow advance into long, transverse surface ridges. These CVP outcrops are bordered by a more or less continuous, narrow zone of OBS, which in turn is surrounded by light-colored FVP. If you have a hand lens, observe the difference in vesicularity between the larger interconnected bubbles of the CVP and the smaller, unconnected bubbles of the FVP. Because of its lower density, outcrops of the CVP tend to ride higher on the flow surface. Heights of the surface ridges also reflect their textural makeup: amplitudes of ridges composed of CVP are commonly higher than those of OBS or FVP. Mapping the distribution of these three textures on the upper surface and flow front of Little Glass Mountain (which we will visit on Day 3) originally led to the idea of a "textural stratigraphy" of rhyolitic obsidian flows (Fink, 1980b).

Flow foliation: Another characteristic of obsidian flow lavas is that they commonly have pervasive flow foliation, made up primarily of aligned microlites. In some cases, layers of vesicles also parallel microlites in pumiceous zones. Flow foliation is most easily observed in samples and outcrops of OBS, but they can also be seen in FVP and CVP. Flow foliation can record deformation of parcels of lava that have risen through the vent, spread downslope, and in some cases moved vertically within the advancing flow. Fink (1983) presented detailed structural maps of the upper surfaces of Little Glass Mountain (for example, fig. 21) that showed a predominance of vertically oriented flow foliation near vent areas, suggesting that foliation preserves shear stress exerted on rising magma parallel to vertical conduit walls. He proposed that the near-vertical orientation of flow foliation persisted as lava moved laterally away from the vent, but that basal shear stresses caused foliation in the lower part of the

flow to gradually rotate to horizontal. This rotation works its way upward through the flow as the lava is transported farther from the vent, but cannot penetrate all the way to the upper flow surface, where foliation orientation tends to be dominated by late-stage processes, especially near the flow front. These include surface folding, the formation of flow-parallel "crease structure" fractures, and the rise of FVP spines and diapirs of CVP.

The evolution of flow foliation will be further discussed at South Sister and Medicine Lake volcanoes, where we will see very small domes that emerged from the same dikes that fed some of the larger obsidian flows. The smallest domes, located immediately above their feeding conduits, don't have the chance to spread very far and thus display almost exclusively vertically oriented flow foliation.

Return to Bend for dinner and hotel.

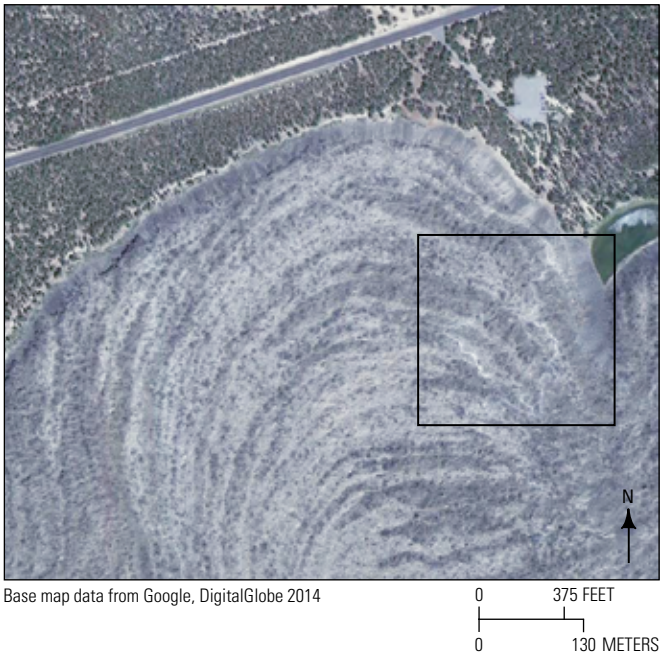

Figure 8. Google Earth image showing distal end of Big Obsidian Flow, Newberry Volcano, displaying three texture types. Finely vesicular pumice (FVP) is the lightest material observed on the surface; darker areas are composed of coarsely vesicular pumice (CVP) and dense obsidian (OBS). These two darker textures are not easily distinguished at map scale, but are evident in the field by examining differences in luster. The area we will traverse is near the right margin of the image where a foot trail provides access to the flow. Note prominent compressional folding is easily identified at this scale, but difficult to discern in the field. Black box shows location of figure 9.

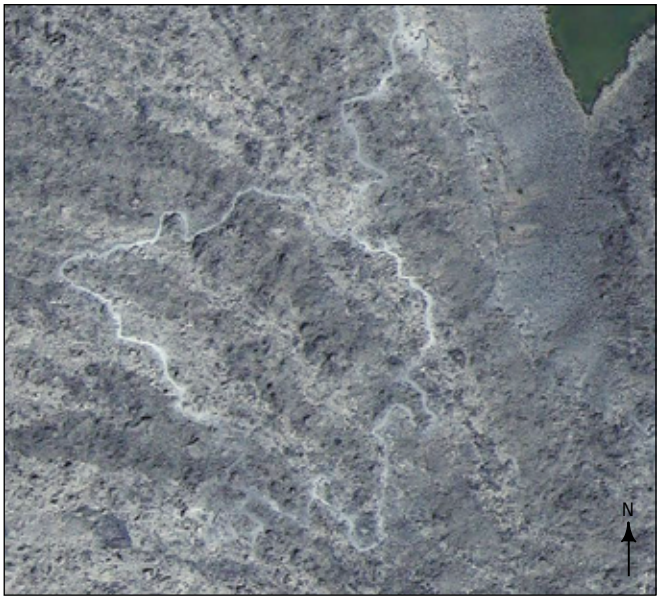

Figure 9. Google Earth image showing closer view of trail on distal end of Big Obsidian Flow. The trail crosses outcrops of coarsely vesicular pumice (CVP), finely vesicular pumice (FVP), and obsidian (OBS), as well as several transverse flow ridges. Note that largest blocks are found in dark areas where CVP has risen diapirically to expose new material at the flow surface.

Day 2—Bend, Oregon, to South Sister Volcano

0.0 Intersection of Mount Washington Drive and Oregon Route 372 (O.R. 372) (Cascade Lakes National Scenic Byway)—Head west on O.R. 372 toward South Sister volcano. **16.1**

16.1 Intersection with U.S. Forest Service Road 45 (NF 45). Stay on O.R. 372 heading west. In the foreground is Mount Bachelor (9,065 ft; 2,763 m), previously named Bachelor Butte. **3.1**

19.2 At Mount Bachelor ski area, stay on O.R. 372 heading west. **1.8**

Mount Bachelor is located at the north end of the 25-km-long Mount Bachelor volcanic chain that contains numerous mafic to andesitic lava flows, cinder cones, and tephras (Scott and Gardner, 1990; Gardner, 1994). The volcanic chain contains nearly 50 vents, with the largest (Mount Bachelor) containing more than 50 percent of the estimated 40 km^3 erupted volume. Most of these features formed during four eruptive episodes over 10,000 years between 18 and 8 ka. Mount Bachelor is a mafic to andesitic cone that sits atop a broader mafic shield, and it grew to nearly its present extent by 11 ka. Ash from Mount Mazama (Crater Lake) overlies all eruptive products in this chain, indicating that all eruptions ceased by 7.6 ka.

The small, reddish cone due west from this vantage point (and due north of the Mount Bachelor summit) is Egan cone. This is likely the site of the last eruption along the Mount Bachelor chain. No soil exists between the Egan cone deposits and the overlying Mazama ash, suggesting Egan cone erupted about 7.6 ka.

21.0 Intersection with NF 370. Continue west on O.R. 372. **2.1**

23.1 Intersection of road to Sparks Lake. Named after pioneer stockman Lige Sparks, this lake was formed about 10 ka (Scott and Gardner, 1990) when lavas from Mount Bachelor impeded the flow of the upper Deschutes River. To the right is South Sister volcano (10,358 ft; 3,157 m) and Broken Top (9,175 ft; 2,797 m). **0.7**

23.8 Cross Fall Creek. **1.0**

24.8 The lowest of the Devils Hill domes comes down to the road, to the right. **0.2**

25.0 Devils Lake on the left, formed as runoff from Hell Creek and Tyee Creek was impeded by older lava flows in the forest on the east shore of the lake. **0.6**

25.6 Entrance to Devils Lake Trailhead parking. Turn left and park.

Stop 1. Devils Lake Trailhead (5,450 ft; 1,661 m)

Today we will hike up the southern flank of South Sister volcano, visit the Devils Hill chain of rhyolite domes, and discuss emplacement of silicic lava through dikes. Hikers will then have two options for the afternoon: option 1, return to the van, retrace our morning drive back to Mount Bachelor, and catch the lift to the top of the mountain to take in views of the Cascade Range and discuss controls on morphology and eruptive style of the Cascade volcanoes; or option 2, continue a strenuous hike to the top of South Sister volcano where far-reaching views of the Cascades await. The two groups will rendezvous in Bend for dinner.

The first 2.5 km of South Sister Climber Trail #36 is deceptively steep, gaining more than 1,200 ft (366 m) through a dense hemlock forest. Outcrops of older glassy rhyolite flows, visible on the ridge east of the trail (fig. 10), preserve radial columnar joints and other fracture patterns interpreted to be evidence of lava-ice interactions (Lescinsky and Fink, 2000).

After emerging from the forest, we enter a pumice-rich plain and come to a four-way trail intersection. Here, we will take a brief side trip west to get a partial overview of Rock Mesa, a large, ovoid, 2.2-ka rhyolitic obsidian flow that exhibits textural variations, prominent surface folds, and a spiny summit dome reminiscent of features seen at Big Obsidian Flow on Newberry Volcano. This part of South Sister was evaluated for geothermal exploitation in the 1970s and 80s. Crustal uplift and extension centered about 5 km west of the South Sister summit began between 1996 and 1998 at a rate of ~4 centimeters per year (cm/yr) and continues at an exponentially decreasing rate (Wicks and others, 2002; Dzurisin and others, 2006, 2009). Total maximum uplift since 1998(?) has been more than 20 centimeters (cm), and the current uplift rate is about 0.4 cm/yr (M. Lisowski, written commun., 2016).

Reversing our path, we will head east to the junction with Moraine Lake Trail. Moraine Lake (fig. 11) sits in a depression surrounded by remnants of older rhyolite flows that also contain evidence of lava-ice interactions. The trail goes eastward along Goose Creek and then passes between some of the smallest Devils Hill lava domes (fig. 12).

Figure 10. Photograph looking northeast showing glassy selvage of older rhyolite flow and fracture pattern interpreted to have formed where flowing lava contacted ice. The distribution of features like these can help determine the extent of glaciation at the time of volcanic activity.

Figure 11. Photograph looking north showing Moraine Lake below summit of South Sister volcano. Devils Hill domes are off to the right (east). Red dashed line shows approximate route to summit.

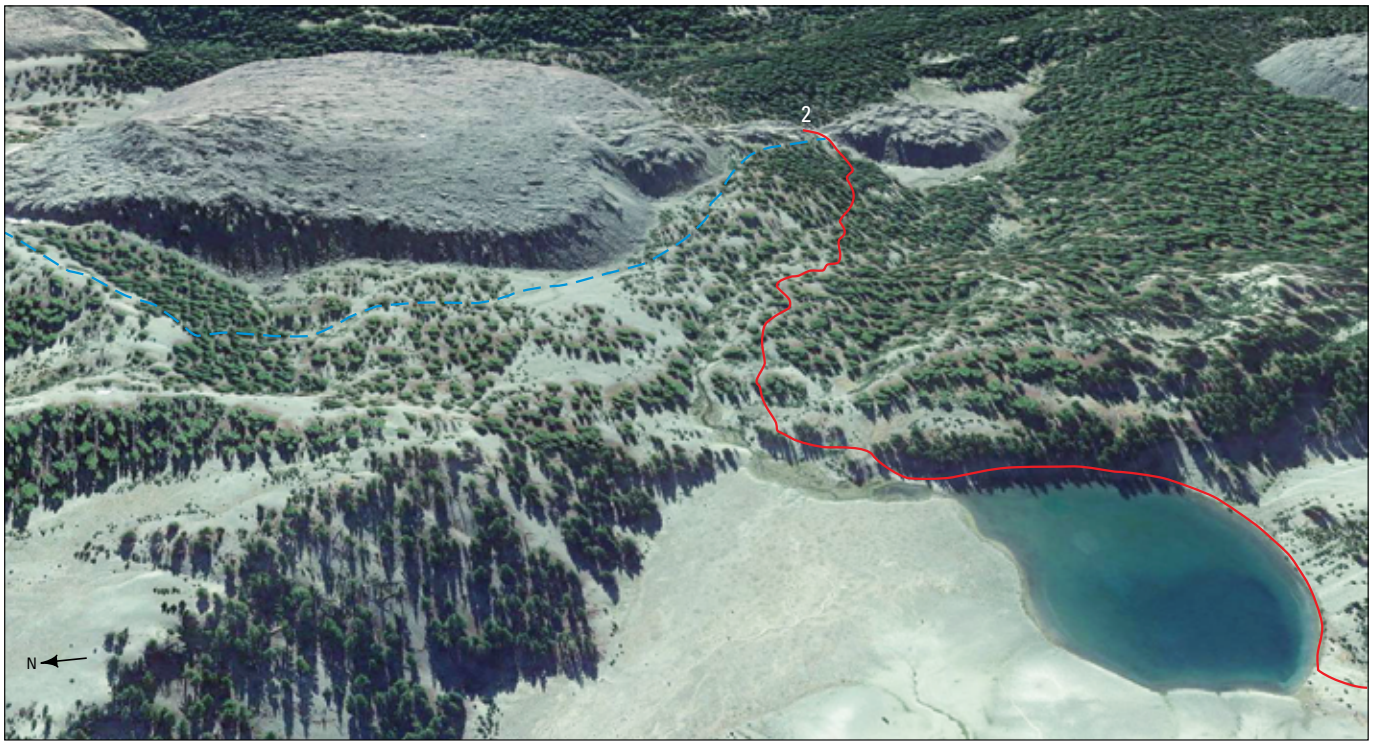

Figure 12. Google Earth image showing oblique view looking east toward Moraine Lake Trail (red line) that passes Moraine Lake and climbs to Devils Hill dome ridge. Stop 2 is shown at end of red line between two very small domes (left and right of the label for Stop 2). Dashed blue line shows subsequent route up along dome trend toward top of Newberry flow to north.

Stop 2. The Devils Hill domes

The Devils Hill chain (fig. 13) is a 5-km-long collection of nearly 20 rhyolitic domes and associated ground cracks and vents that formed during the most recent eruptive cycle at South Sister volcano (2 ka; Scott, 1987). Most of the erupted volume emanated from one of the highest vents in this chain and formed the prominent Newberry flow. Some domes in the Devils Hill chain are less than 10 m high and 50 m in diameter.

Most well-studied rhyolitic obsidian domes and flows are assumed to be dike fed, and the Devils Hill chain is one of the best examples of this emplacement style. Our understanding of rhyolite dike intrusion processes comes largely through analogy with observations of recent and prehistoric basaltic eruptions, the latter exposed by erosion. Fissure-fed basaltic eruptions begin with a "curtain of fire" phase, during which magma can erupt from a several-kilometer-long series of linear vents. Relatively quickly (within hours to days), magma moving through the narrower ends of a dike begins to cool and solidify, causing the eruption to localize in one or two wider areas near the center of the dike. These wider areas can supply an eruption with magma for days, weeks, or years. Large volumes of lava are assumed to be associated with the thick parts of dike segments, because these areas remain hot longer and allow more magma to erupt before cooling and crystallizing. (Delaney and Pollard, 1981).

Silicic dikes associated with composite volcanoes like South Sister are inferred to be straight and continuous at depth, but as they approach the surface, they encounter rotating stress fields and variable host-rock rheological properties, either of which can cause the dike to break into segments (Delaney and Pollard, 1981; Fink, 1985; Reches and Fink, 1988; Fink and Anderson, 2000). These dike segments in turn can rotate relative to the overall trend, leading to en echelon patterns. Aligned dome groups, flow bands and fractures preserved in lavas near dome vent areas, and elongate shapes of small domes all help constrain the geometry of the subsurface magma plumbing system.

Geomorphic and textural features in the Devils Hill chain include small en echelon offsets of individual dike segments, asymmetric and elongate dome shapes, and aligned flow foliation (fig. 13). It is not known whether the dike (or dikes) rose vertically from magma reservoirs beneath the dome trend, or if they emerged obliquely from beneath the center and summit of South Sister volcano. Gravity data failed to detect subsurface positions of dikes between some domes, likely because of a lack of density contrast between the intrusive and

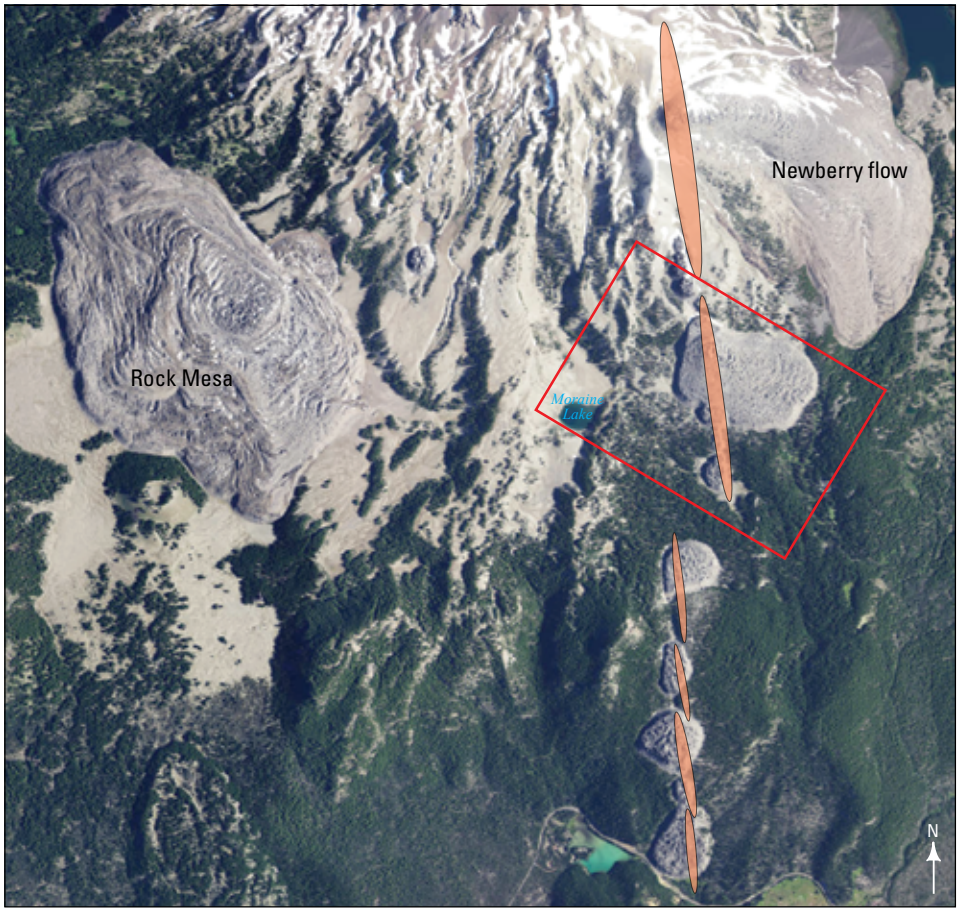

Figure 13. Image showing south flank of South Sister volcano, and Rock Mesa (west) and Devils Hill (east) domes. Orange ellipses mark positions and orientations of en echelon dike segments assumed to have fed the domes, inferred on the basis of dome shape, nearby ground cracks and depressions, and lava flow banding. Our parking area is shown along the bottom edge of the image, west of the small blue-green lake. Moraine Lake is slightly right of center in this image. Red rectangle shows location of figure 12.

0 1 2 3 KILOMETERS
0 1 MILE

surrounding country rocks (C.R. Manley and J.H. Fink, unpublished data, 1984).

Additional insights into silicic dike emplacement come from studies of the deeply eroded remains of Summer Coon, an Oligocene volcano in south central Colorado that is assumed to have been roughly circular in plan view, with a diameter of about 20 km (Lipman, 1968). A radial suite of well-exposed rhyolite, rhyodacite, and andesite dikes extending from the presumed center of the volcano to its preserved outer slopes shows evidence of flow foliations developed during magma flow. Poland and others (2004) mapped these dike trends, along with paleomagnetic measurements, and concluded that the magma likely rose vertically until it reached a level of neutral buoyancy, and then flowed laterally until it intersected the flanks of the volcano where it erupted as lava (fig. 14). Remnants of the dikes and the lava flows they fed are preserved in outcrops.

The Moraine Lake Trail intersects the Devils Hill chain in the middle of a group of several domes, most of which are very small. We'll spend some time here, both on and off the domes, looking for evidence of dike structure. The northernmost dome in this local group is the second largest along the Devils Hill chain. Does extrusion volume depend mostly on feeder dike thickness, or might large flows occur in parts of the volcano where the edifice has additional zones of weakness that allow magma to reach the surface more easily? From a textural standpoint, how do the surfaces of these very small domes compare with the more complex surface of Big Obsidian Flow? Do lava textures depend mostly on magmatic volatile content, eruption rate, conduit wall permeability, or distribution of pre- or post-eruption shear stresses? If volatiles are distributed in a nonuniform way, are variations zoned vertically or horizontally in a dike?

How much lateral flow is involved in a dike-fed dome eruption? In other words, does magma sample the conduit directly below a dike, or is some lateral flow and associated mixing involved? If a dike contains a heterogeneous distribution of volatiles or other chemical constituents, how do those mix as magma moves through the dike? Can we still infer the original chemical makeup of the source magma body from erupted or intruded products if we don't understand these dynamic processes? We walk along the flanks of South Sister volcano and infer the

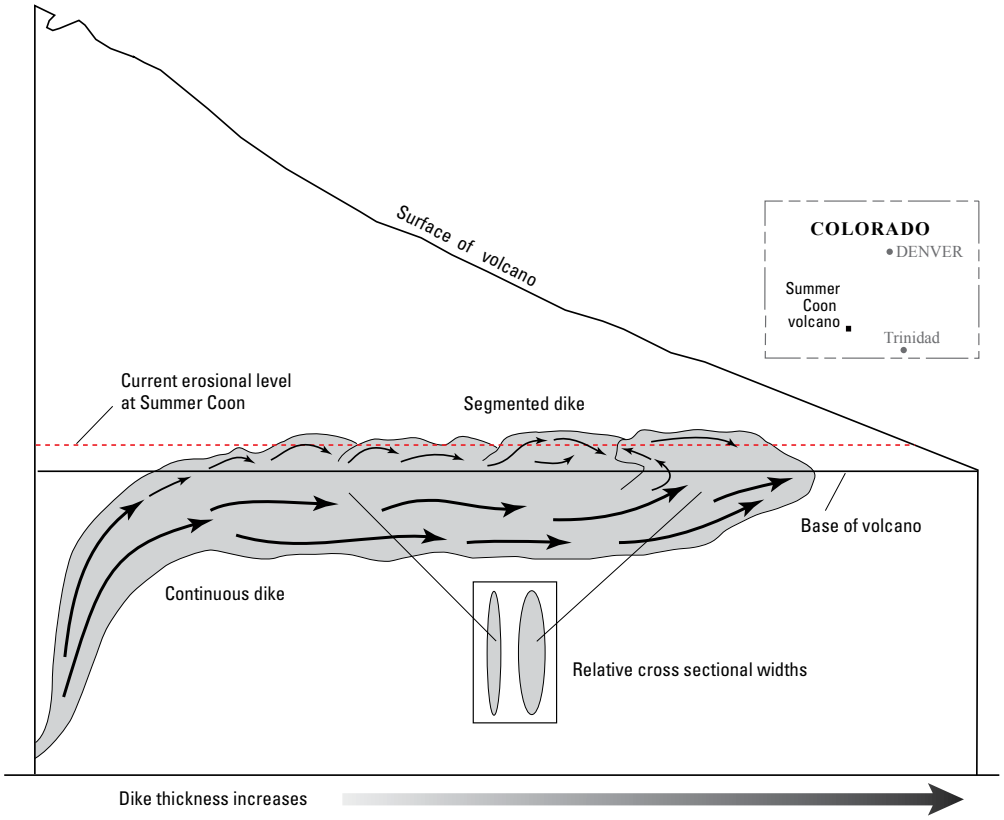

Figure 14. Schematic radial cross section of inferred silicic dike geometry at Summer Coon volcano, south-central Colorado. Arrows show lateral magma flow toward volcano flank. From Poland and others, 2008.

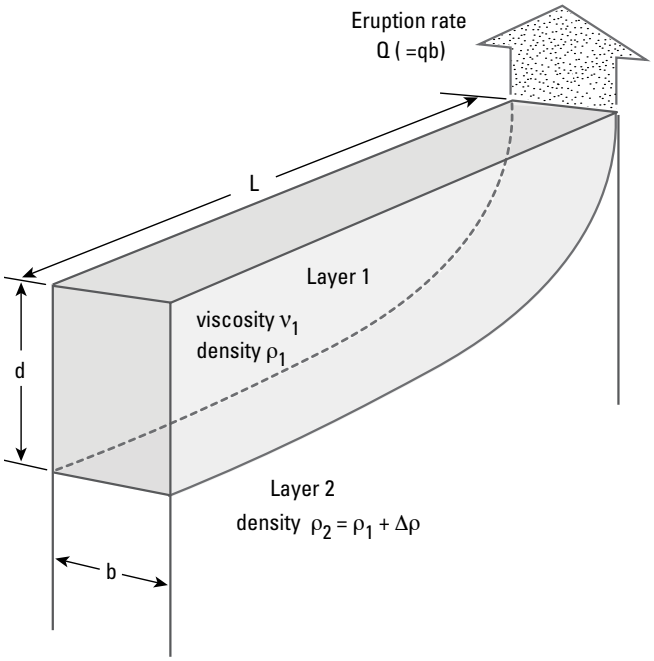

Figure 15. Schematic diagram showing magma withdrawal from a vertically stratified dike of width b and length L. Layer 1, of depth d, has density ρ_1 and viscosity ν_1. Layer 2 has a higher density (ρ_2) than Layer 1, with the difference being $\Delta\rho$. Depending on eruption rate (Q), dike geometry, and the physical properties of the two fluids, the eruption may sample one or both layers. q is eruption rate per unit width b. Adapted from Blake and Fink, 1987.

magmatic processes that are happening (or happened) beneath the surface. In contrast, at Summer Coon volcano, we would walk along the once-buried dike and infer magmatic processes from the now-eroded paleosurface.

The silicic lavas that make up the Devils Hill chain have uniform chemistry, at least as far as major elements. At other dike-fed silicic extrusion sites, most notably the Inyo dome chain of eastern California and Glass Mountain at Medicine Lake, domes and the Plinian deposits that precede them can have as many as three distinct chemical end members preserved in dikes, tephras, and subsequent lava flows. Motivated by the complex geochemical mixing observed in the Inyo dome chain, Blake and Fink (1987) presented laboratory simulations and a mathematical analysis of the dynamics of magma withdrawal from a stratified silicic dike. Figure 15, adapted from their paper, shows a hypothetical two-layer fluid in a slot subject to critical draw up, as might be the case for magma withdrawal from a stratified silicic dike. The greater the eruption rate, the deeper and laterally further from the vent that eruptible magma can be drawn. This finding suggests that, while uniform lava composition along a dome chain may indicate a homogeneous source, it could also represent an eruption rate too low to tap vertically stratified layers.

After looking at this first set of small domes (fig. 16), we'll scramble northward up the scree slope to the west to look at four smaller domes in a graben south of the Newberry flow (fig. 17). Here we will examine the fractures that dissect the tiny domes. Some of the most prominent cracks run perpendicular to the dome group trend. What mechanism formed these cracks? How would these petite extrusions transition into larger domes and flows if their eruption had continued longer? What kinds of geochemical variations should we expect to find among these small "domelets"? What geophysical or remote-sensing measurements might shed light on the subterranean structure of these vents? What answers might laboratory simulations of silicic eruptive processes provide? If we had the opportunity to observe a set of dike-fed domes while they were active, what measurements would be the top priority, and what fundamental questions about magma genesis, volcanic hazards, or geothermal resources might these sightings permit us to address?

From the edge of the small set of domes, we'll make our way east to get a good overview of the west side of the Newberry flow. This flow is morphologically similar to Big Obsidian Flow, but like all of the South Sister domes, it has less textural variation and less obvious glass than its counterparts at Newberry. This brings up the question of why silicic extrusions on volcanoes along the main Cascade axis appear less glassy than those found on the Newberry and Medicine Lake volcanoes 20–30 km to the east. Does the off-axis extensional tectonic regime make it easier for rhyolite to develop without mixing to form rhyodacite, dacite, or andesite? Has the lack of pervasive compressive stress allowed rhyolite dikes to surface rather than cooling and crystallizing as subsurface dikes?

Figure 16. Image showing small aligned domes along Devils Hill trend. Determining what constitutes an individual dome is not straightforward. The smallest domes here and immediately to the north (fig. 17) may represent the top of a dike that ceased erupting as soon as lava breached the surface.

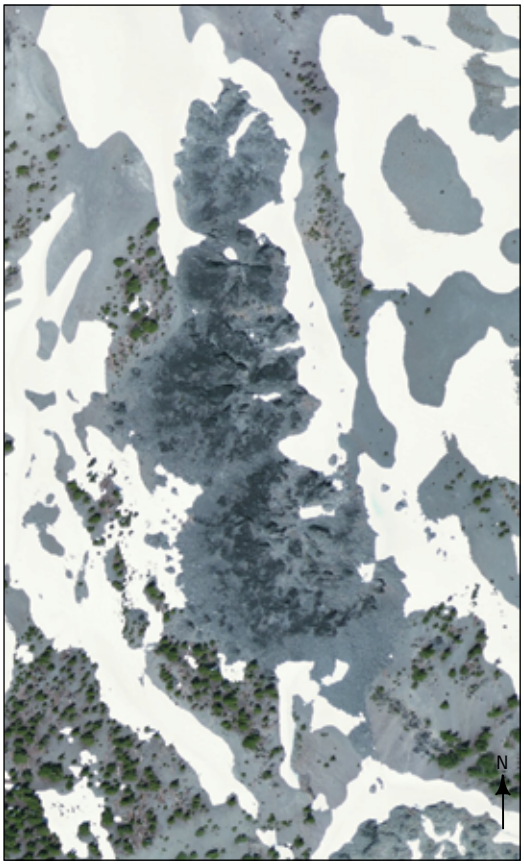

Figure 17. Image showing small domes south of Newberry flow vent, Devils Hill dome chain. These domes underwent virtually no lateral flow after emerging from their vents, which are presumed to have been at the top of a dike.

After this stop, Mount Bachelor visitors will retrace their steps back to the van. If the weather appears threatening, all will head down to the van and travel to Mount Bachelor. If not, summit hikers will return to the intersection of trails west of Moraine Lake, and follow the trail uphill for 2.1 km where it intersects the summit trail, and then another 3.7 km of difficult trail, climbing 950 m to the summit (fig. 18). There is a false summit 1.8 km from the top where we will see Lewis Glacier on the right, and Clark Glacier on the left. As we approach the summit, we will look down on Teardrop Pool to the left, the highest lake in Oregon.

We will then return to the vans, staying right at the trail intersection 3.7 km from the summit and avoiding the lengthy traverse around Moraine Lake that we took on the way up.

All participants will meet back at the Devils Lake Trailhead late in the day and return to Bend for dinner and to spend the night.

Figure 18. Topographic map of the South Sister volcano summit area. Black dashed line shows trail to summit. Grid = 1 kilometer.

Day 3—Bend, Oregon, to Klamath Falls, Oregon, and West Side of Medicine Lake Volcano

0.0 Intersection of U.S. 97 and U.S. Forest Service Road 18 (NF 18; China Hat Road). **6.5**

6.5 Lava Butte to the west with an accompanying basaltic lava flow. This cinder cone and flow is part of a group of small cones on the northwest flank of Newberry Volcano (see fig. 3). **46.4**

52.9 Intersection with Oregon Route 58 (O.R. 58). **27.7**

80.6 Mount Mazama/Crater Lake is approximately 20 km due west of this point. **49.0**

129.6 Intersection of U.S. 97 and Oregon Route 39 (O.R. 39) in Klamath Falls. **17.4**

147.0 Dorris, California. **10.6**

157.6 Macdoel, California—Turn left onto Old State Highway. **1.0**

158.6 Turn left onto Red Rock Road, which becomes Davis Road, and is also called U.S. Forest Service Road 45 N 05 (USFS 45 N 05) and the "Tennant Lava Beds Road" on Google Maps. **16.5**

175.1 Intersection with Harris Springs Road (USFS 45 N 05). To the east is Medicine Lake volcano (fig. 19). As a result of its off-axis location and large volume, this volcano has some morphological similarities with Newberry Volcano. Both lack the high, pronounced summits commonly found in the on-axis Cascade volcanoes. At Medicine Lake, recent eruptive vents are spread over a broad area and produced flows that span a wide compositional range. Donnelly-Nolan and others (2008, 2016) provide a comprehensive geologic history of Medicine Lake volcano. **14.4**

189.5 Turn left onto U.S. Forest Service Road 43 N 77 (USFS Road 43 N 77). **0.7**

190.2 On the right is the flow margin of Little Glass Mountain (fig. 20). Little Glass Mountain is actually composed of two rhyolitic flows that display the three primary lava textures (FVP, OBS, and CVP), along with structures such as compressional folds that help constrain the timing of textural development. The main flow is as much as 100 m thick in some places and areally extensive (8–9 km^2). We will visit the northwest and northeast lobes of this flow to see well-developed textural contrasts and structures, and then continue on to a vantage point at the summit of Little

Figure 19. Image showing aerial view of Medicine Lake volcano and prominent Holocene lava flows and their compositions (A, andesite; B, basalt; BA, basaltic andesite; D, dacite; R, rhyolite). Medicine Lake (labeled in white) is located roughly in the center of the summit caldera. We will visit the rhyolite and dacite flows shown in the figure.

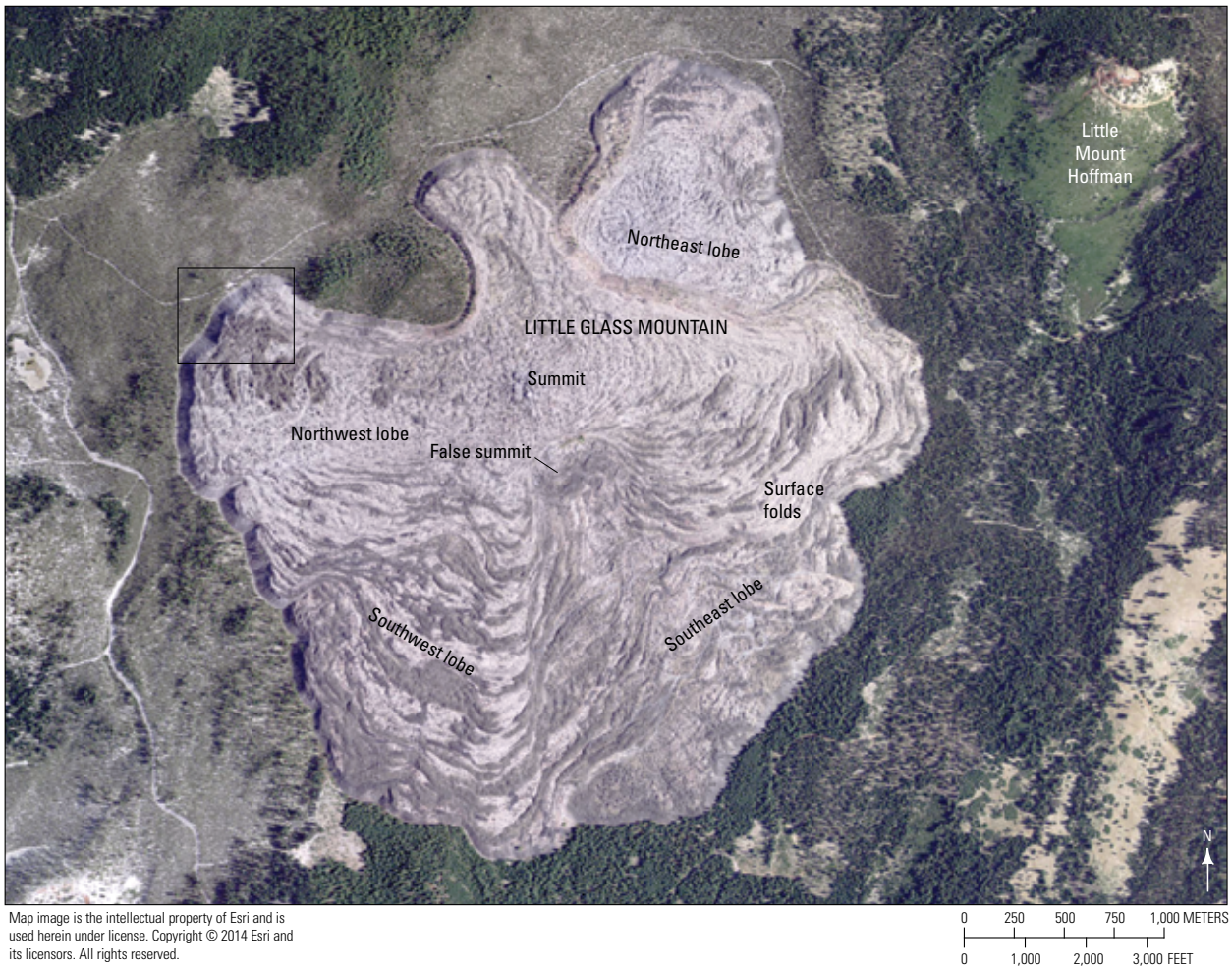

Figure 20. Image showing aerial view of Little Glass Mountain, light finely vesicular pumice (FVP) textures, and dark obsidian (OBS) and coarsely vesicular pumice (CVP) textures. Note that dark textures are clearly deformed by surface folding suggesting that CVP rose to the flow surface diapirically before the end of flow emplacement. We will visit the northeast lobe and the flow front of the northwest lobe to observe deformed diapirs of CVP along with the crease structures that bisect them. Black box shows location of map in figure 21.

Mount Hoffman where we can look down over the entire flow surface. **3.1**

Stop 1. Northwest lobe, Little Glass Mountain

The northwest lobe of Little Glass Mountain has a very steep and tall flow front. Climbing up the scree can be challenging, especially for a group. Consequently, we will look up at this flow front from below and examine the large blocks that cover the area. These views will introduce us to the geometry of the three primary textures in the flow front: FVP, OBS, and CVP. We will present a description of the upper surface of the northwest lobe, which you are welcome to observe on a future trip. If you do ascend, do so diagonally so that there is not somebody directly below you, as you will likely dislodge many loose blocks. It is recommended that you wear gloves while climbing.

Once on top of the flow, you can see extensive, relatively smooth surfaces that are the "wings" of a few prominent CVP diapirs. You can explore and interpret these features, looking for evidence of how they formed. In some places it is possible to see distinctive small folds that developed during rise of the diapirs, which were subsequently fractured; two halves of the same feature can be seen on opposing walls of the large fracture, in some cases 5 m or more apart. It is also possible to find sites where fracturing occurred in multiple stages, with the early smooth surface being refractured by a second pulse of extension of a different orientation. We refer to these fractures as "crease structures" (Anderson and Fink, 1992); they develop on parts of the flow surface that are undergoing extension. Here on the northwest lobe, extension resulted from lateral spreading of the advancing flow and upward doming of buoyant CVP diapirs. In other places, such as the north lobe of nearby

("Big") Glass Mountain, extension was localized along folded surface ridges, perpendicular to flow direction, again resulting in crease structure axes that parallel flow advance. Crease structures vary greatly in size and their long axes can measure from less than 3 m to more than 250 m. In fact, the entire surface of some extrusions, like the October 1980 lobe of the Mount St. Helens dome, consists of a single crease structure. U.S. Geological Survey workers at Mount St. Helens informally referred to these features as "babies' butts."

The entire CVP zone is roughly encircled by a narrow band of OBS, although this can be difficult to detect. If one walks upslope toward the vent, the CVP outcrops become smaller and more equant, separated by spacing that has been attributed to Raleigh-Taylor instability associated with buoyancy of the volatile-rich interior zone that forms the CVP (Fink, 1980b). Flow banding in the CVP and surrounding outcrops reveals a dome-like, doubly plunging anticlinal structure; this pattern is what originally led to the interpretation of the CVP forming buoyant diapirs.

The structural map and cross section shown in figure 21 are derived from measurements of flow banding orientations in CVP, OBS, and FVP outcrops (Fink, 1983). Transverse anticlinal ridges cut by longitudinal fractures dominate the structure. Obsidian outcrop selvages located between adjacent parallel diapirs form tight synclines, as shown in the cross

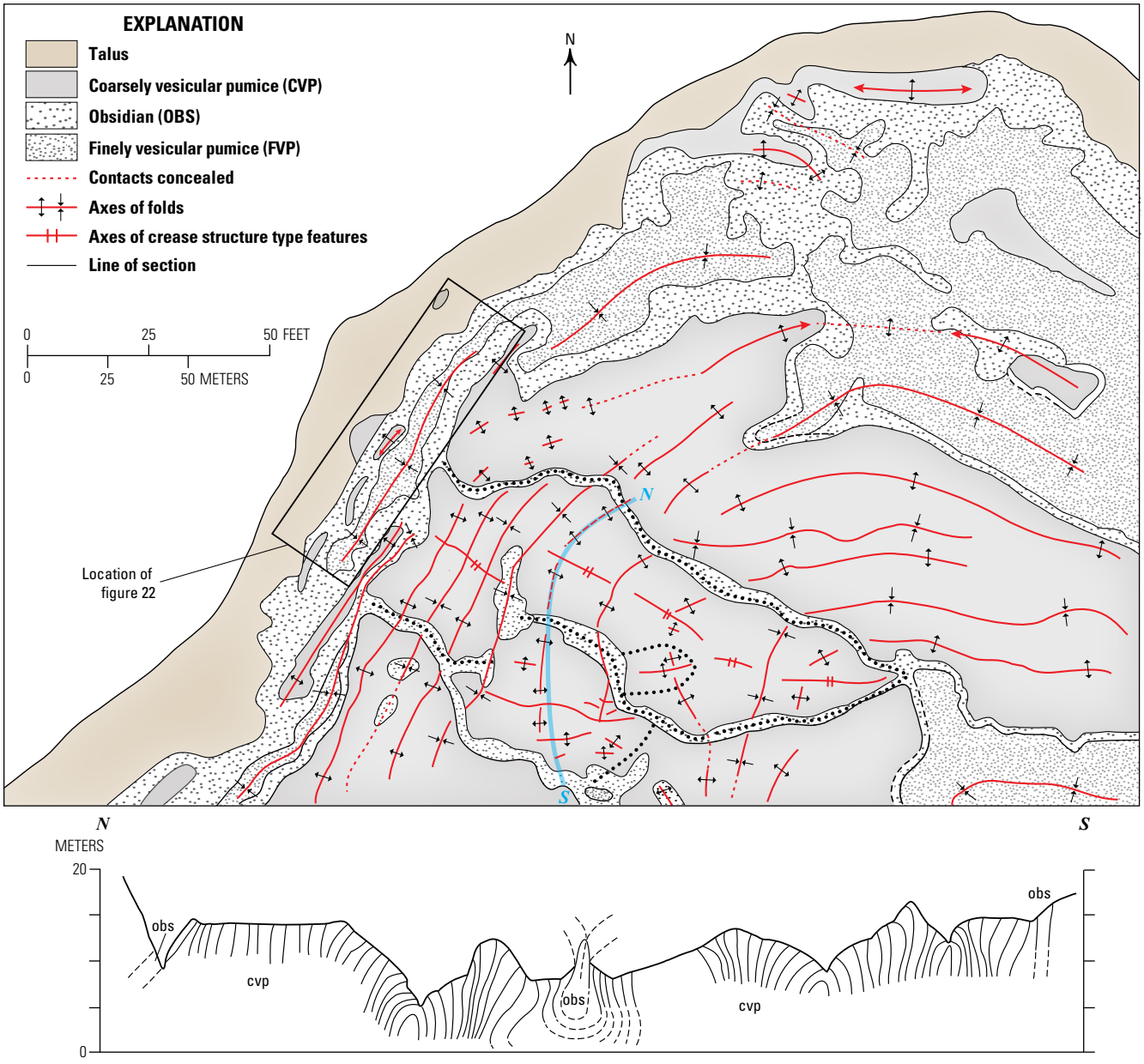

Figure 21. Structural map and cross section of coarsely vesicular pumice (CVP) diapir area on northwest lobe of Little Glass Mountain. Curving north-south cross section (thick blue line) cuts across lower middle part of map. Black box shows location of figure 22. Modified from Fink (1983).

section. The two photographs in figure 22 show the anticline in the flow front, which plunges into the flow interior. This structure can be seen from below. Large, stretched vesicles in the CVP reflect outward bulging of the outcrop as it was emplaced into the flow front. Bordering obsidian outcrops help define the structure of the anticline. Large vesiculated blocks, as much as 1 m long on a side, which fell from these outcrops, can be examined at the base of the talus slope.

A question to ask while looking at this part of the flow is how the physical properties of the CVP evolved as the texture was forming and deforming. Was the CVP more or less viscous than the less bubbly OBS zones above and below it? When did the bubbles that formed the observed vesicles start and stop growing? How and when did the fracture surfaces develop? We will see even better preserved microstructures on crease structures at the Medicine Lake Glass Flow.

Another question to consider is whether any of these geologic features deserve or require protection so that they are not removed by pumice mining operations. Obsidian Dome in the Inyo dome chain of eastern California has one of the world's most dramatically exposed CVP diapirs, which has been partially removed by pumice mining over the past two decades. Students will never have the opportunity to learn from those parts of the outcrops that have now been ground up and consumed by manufacturers of concrete or cinder blocks. *Geopark* (UNESCO, 2016), or some similar designation, might offer long-term protection to key geologic features such as the ones we are seeing on this field trip.

Stop 2. Northeast lobe, Little Glass Mountain

Little Glass Mountain has three distinct summit areas (fig. 20). The highest part of Little Glass Mountain is a broad, ill-defined domal area filled with large blocky outcrops. Immediately to the south is a very dark, steep-sided structure (referred to as "false summit" on figure 20) around which are draped laterally extensive, transverse surface folds (remnants of a single-engine plane that crashed into this part of the flow in the 1970s can still be found). The pattern of flow ridges on this steep-sided structure suggests that this dark bluff rose up through the advancing lava—some of the earlier formed, more distal folds in the southeast and southwest lobes connect across the southeastern part of this structure, whereas later flow ridges, farther upslope and closer to the top of the steep-sided structure, are bent and broken. These views convey the highly fluidal behavior of this very viscous lava.

The northeast lobe has a roughly circular, light-colored vent area, cut by prominent radial fractures. This lobe is a distinct lava flow that emerged, likely from the same dike, before the rest of Little Glass Mountain, and was later overridden on its southwestern margin. The northeast lobe contains many of the features of the main flow in more accessible, miniature form; its flow fronts are not as high, and the CVP diapirs and surface ridges are less well developed. We will visit a small well-exposed CVP diapir cut by a crease structure and surrounded by outwardly dipping outcrops of OBS and FVP. We will also see spines that grade from OBS at their base to FVP at their top. Several of these spines have pink surface coatings of finely comminuted ash particles (fig. 23). Based on observations of the Cordón Caulle Flow, these ash particle surfaces are now interpreted to represent places where pyroclastic venting occurred during lava emplacement.

If time permits, we will hike toward the summit area of this lobe to see deep fractures, large blocks, and

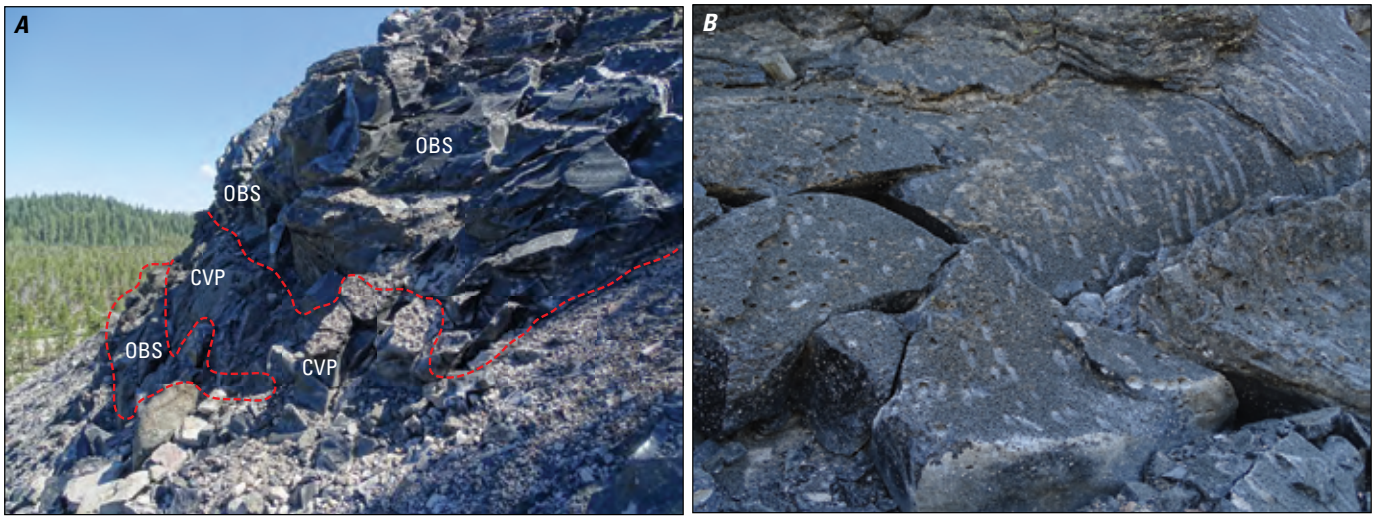

Figure 22. Photographs looking north showing plunging anticline seen in flow front of northwest lobe of Little Glass Mountain. *A*, Coarsely vesicular pumice (CVP) bordered by obsidian (OBS). *B*, Note large stretched vesicles visible in the right side of photograph.

an unusually smooth, folded outcrop of microvesicular rhyolite typical of the vent parts of some of these extrusions.

We will park the vehicles where the flow comes closest to the road (fig. 24). Looking at the flow front here, one can see a well-defined band of CVP separated from the FVP carapace by irregular outcrops of OBS. We will climb up the part of the flow front that has the most FVP, which tends to be the most stable. Here again, be careful about dislodging loose blocks onto your fellow climbers. Once on the flow surface, we will head for a prominent, isolated, elongate crease structure in a CVP outcrop about 5 m from the flow front.

This part of Little Glass Mountain is the first place where surface structures and textures of an obsidian flow were mapped in any detail. Imagine that you are a geology graduate student wandering around trying to make sense of the jumble of multihued blocks scattered across the flow. At the time this flow was mapped, there were no descriptions of glassy rhyolite surface textures

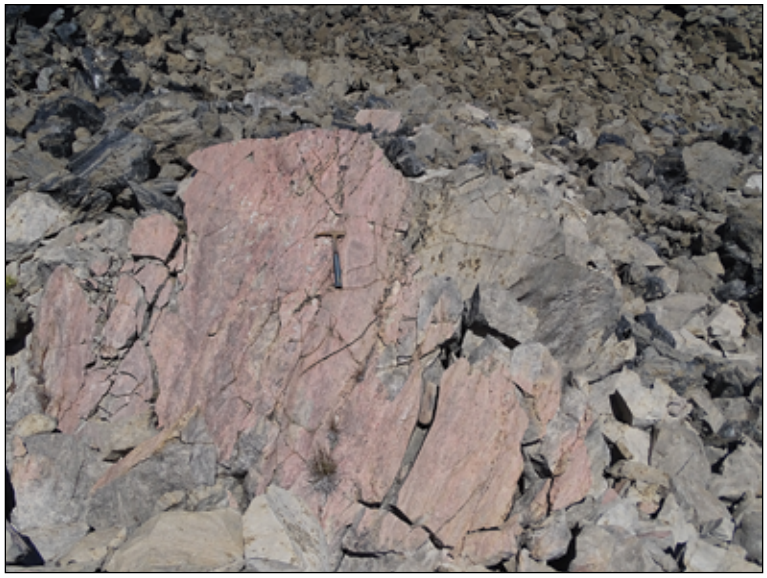

Figure 23. Photograph showing pink coating on block surface interpreted to be evidence of gas jetting during lava flow advance.

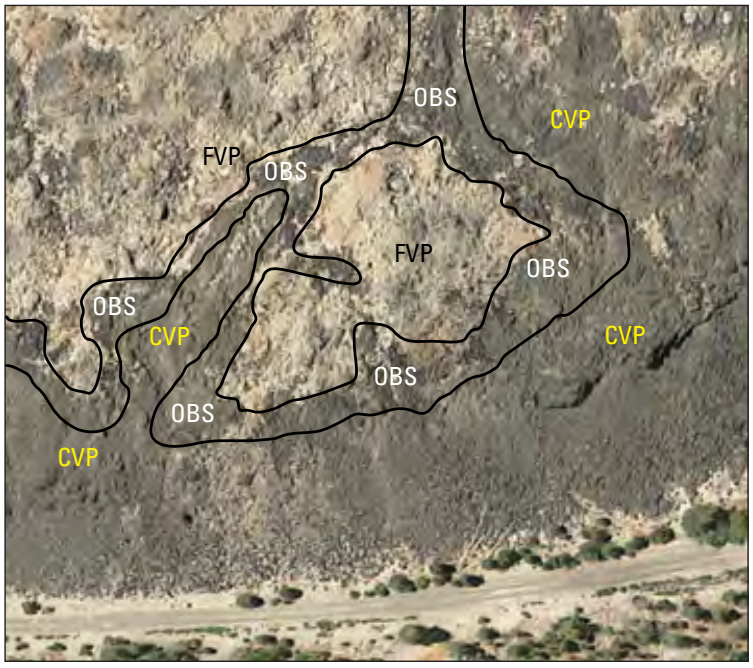

Figure 24. Google Earth image showing northeast margin of northeast lobe of Little Glass Mountain, with north to the right, showing coarsely vesicular pumice (CVP), obsidian (OBS), and finely vesicular pumice (FVP) outcrops. Prominent crease structure cuts through diagonally oriented outcrop of CVP shown in left center of image. Blocks of FVP lying in the crease axis presumably landed there as the fracture was opening up. Note that CVP outcrop gives way to OBS toward its upper right apex.

or structures in the literature, no sense of "textural stratigraphy," and no models for how any of these features developed. This small CVP outcrop helped unlock the puzzle. Flow banding in the surrounding OBS outcrops revealed a consistent dome-like pattern, and the contacts separating OBS from CVP on one side and OBS from FVP on the other side, suggested a doubly plunging anticlinal structure cut by a medial fracture. These observations suggested that the blocks of FVP along the central axis were remnants of a surface layer that had been broken and shoved aside by rising, buoyant CVP. Many pieces of the story we're telling on this field trip took a few decades to decipher, but this outcrop is where our knowledge of silicic flow emplacement first started to come together.

In contrast with CVP formation, vesiculation of FVP appears to be a simpler process: lack of pressure at the upper flow surface allows the small amount of magmatic water in the glassy OBS lava to effervesce. The water content in the OBS is assumed to be largely magmatic, whereas that in the FVP is more likely to have been contaminated at low temperatures by meteoric water percolating into vesicles during hundreds of years of surface exposure. Because solubility in lava is pressure dependent, magmatic water content likely increases as pressure increases toward the flow interior and could reach a critical value large enough to explosively decompress to form explosion pits (fig. 44) or pyroclastic flows during flow front collapse.

To test whether magmatic water content increases (and at what rate) toward the flow interior, one must distinguish magmatic water from meteoric water; this can be done by using step-heated isotopic analyses through which samples are incrementally heated, and the water driven off at specific temperatures is isotopically analyzed. The assumption is that the temperature at which the water leaves the sample is the same as the temperature at which it was incorporated into the lava.

Step-heated isotopic analysis was used on samples from this part of the northeast lobe. Four samples collected from a 2-m-tall spine that grades from OBS at the base to FVP at the top (fig. 25) were analyzed for water content and hydrogen isotopic composition (δD). Analysis revealed that the high water content of the FVP was almost entirely meteoric, whereas the lower water content of the OBS was all magmatic. DeGroat-Nelson and others (2001) used this

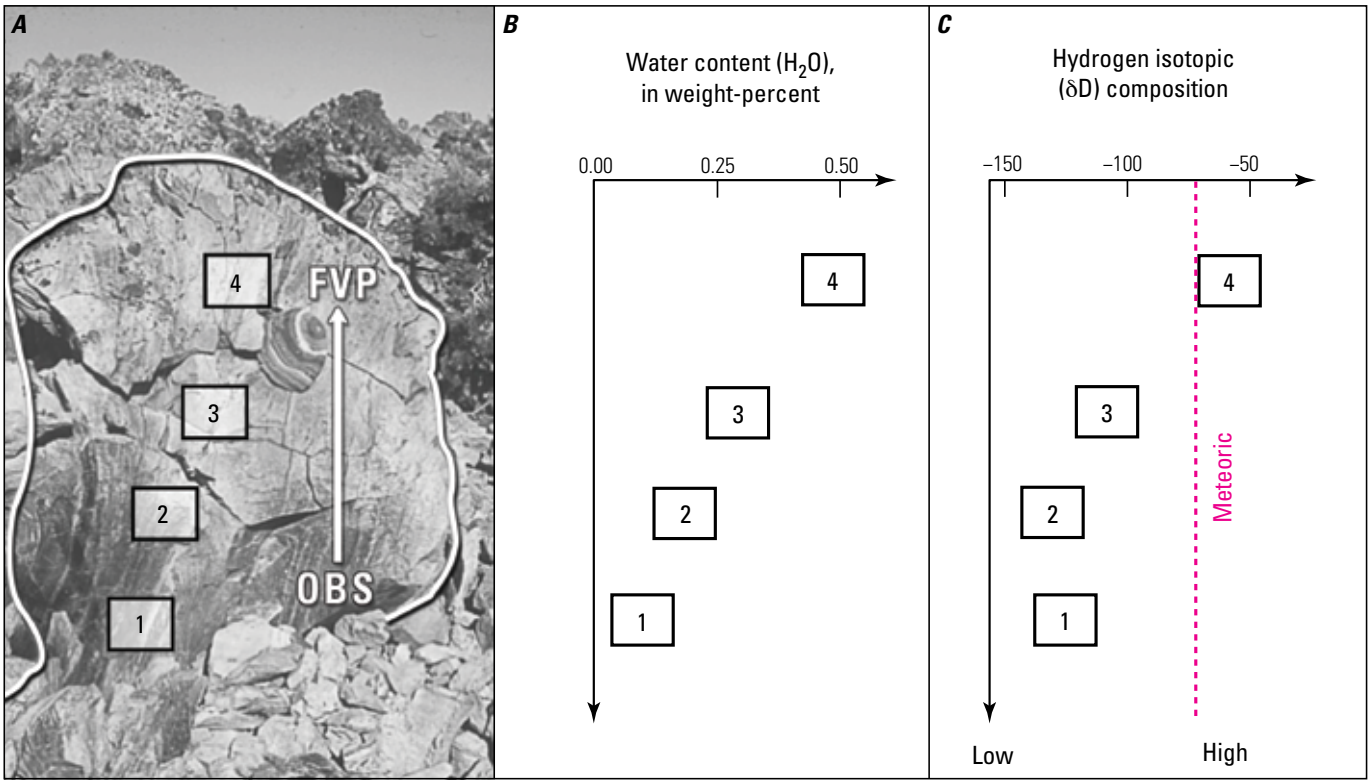

Figure 25. Photograph and graphs showing sample locations and water content data from a spine located on northeast lobe of Little Glass Mountain, with obsidian (OBS) at the base grading to finely vesicular pumice (FVP) at the top. *A*, Photograph showing where four samples were collected from the spine for isotopic analyses. *B*, Graph showing water content of the four samples (in weight percent). *C*, Graph showing hydrogen isotopic composition of the samples (δD). Higher (less negative) δD values correspond to meteoric water, which is assumed to have been added through hydration. From DeGroat-Nelson and others, 2001.

approach to show that residual magmatic water content increased steadily toward the flow interior, resulting in volatile pressures at depths of ~10 m that could exceed the strength of the surface crust.

For visitors with more time, the northeast lobe also offers an excellent opportunity to examine the fractured summit of a glassy rhyolite flow. From the CVP diapir that was just viewed, walk about 600 m south-southwest, toward the area where the flow is buried beneath the southeast lobe flow front (fig. 26). Along this route, you can see radially oriented, rift-like valleys as much as 5 m deep extending toward the apex of the northeast lobe. The lava in this central vent area, which makes up more than two thirds of the area of the overall flow, mostly exhibits a different appearance from the CVP, OBS, and FVP. It is white to pinkish grey (like the FVP), but has a more uniform microcrystalline texture and smaller vesicles than the FVP. Foliation tends to be steeply inclined, especially near the base of the deep valleys. This part of the flow is separated from the more heterogeneous marginal area by a break in slope, with the outer area having less topographic relief but more textural variety.

Just before reaching the talus slope that defines the southeast lobe, there is an unusually smooth area that has been compressed into surface folds unlike those on any other rhyolite flow we will see (fig. 27; Fink 1983). The long axes of the folds are perpendicular to apparent flow direction, suggesting that they formed by flow-parallel compression. Flow foliations are all near vertical and the steep-walled troughs between the folds have V-shaped profiles. If this vertical flow foliation formed during flow through the conduit, then it would have had to be transported laterally away from the vent without significant rotation.

Head east from this location, parallel to the southeast lobe flow front, back to the road.

193.3 Turn right onto Little Mount Hoffman Road. **0.6**

193.9 Park along the road near the summit. **0.6**

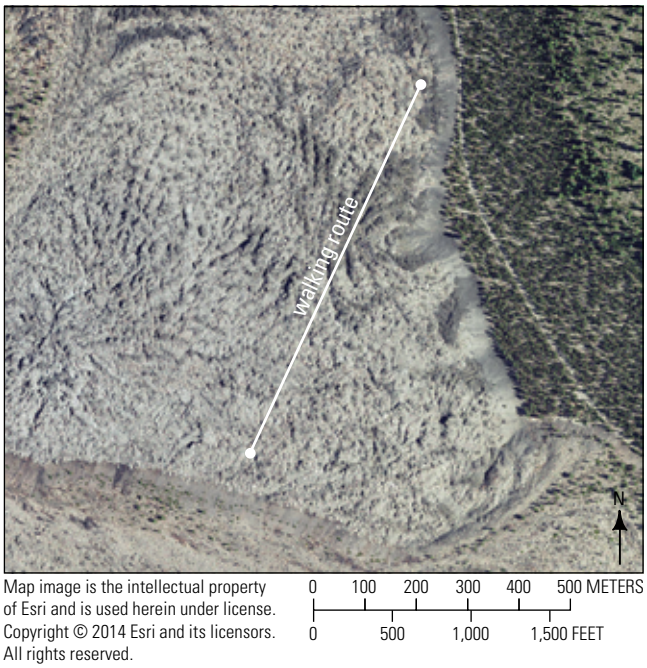

Figure 26. Image showing northeast lobe of Little Glass Mountain and approximate route to walk from a coarsely vesicular pumice (CVP) diapir that was just visited, to a folded, smooth fracture surface on edge of summit area. Note radial fractures coming out from highest point on lobe (lower left corner of image).

Figure 27. Photograph showing surface folds on edge of summit area, northeast lobe, Little Glass Mountain. Fold spacing (wavelength) is about 3 meters (m) and height (amplitude) is about 1.5 m. Flow bands in microcrystalline rhyolite are oriented generally parallel to the long axes of the folds and steeply inclined. Steep slope in the background is the southeast lobe flow front of Little Glass Mountain, which postdated and overrode the northeast lobe in this area.

Stop 3. Little Mount Hoffman

Little Mount Hoffman is one of many Pleistocene basaltic (52 percent SiO_2) cinder cones on Medicine Lake volcano. From this vantage point we have dramatic views of Mount Shasta dominating the western horizon (fig. 28*A*), and Little Glass Mountain in the foreground. Mount Shasta is an andesitic to dacitic stratovolcano with an elevation of 4,317 m (14,163 ft). It last erupted in 1786 (Miller, 1980). Large blocky andesite flows and one of the most areally extensive landslides on Earth (440 km^2; Crandall, 1989) dominate its north flank.

This view of Little Glass Mountain is occupied by the earlier erupted northeast lobe, which we just visited (fig. 28*A*). CVP outcrops are visible along the eastern and northern flow fronts of the northeast lobe, and its broad, deeply fractured, dome-like vent area can be seen toward the southwest. On the southeast lobe of Little Glass Mountain (fig. 28*B*) are prominent surface ridges, several of which are made of CVP. Assuming that CVP reached the flow surface as diapirs, their presence in the flow ridges indicates that they emerged during flow surface advance. Overall, CVP is better developed on Little Glass Mountain than on any of the Newberry or South Sister silicic flows.

As we have discussed, it can be difficult to distinguish vesicular textures while walking across the surface of a rhyolite flow. An alternative approach developed by Ramsey and Fink (1999) uses thermal infrared remote sensing to map the areal percentage of vesicles in flow surface samples on the basis of emissivity. Figure 29 shows two maps of Little Glass Mountain in which different degrees of vesicularity have been color coded, representing resolutions that correspond to the Thermal Infrared Multispectral

Figure 28. Photographs showing views from the summit of Little Mount Hoffman looking southwest (*A*) and south (*B*). *A*, Summit and northeast lobe of Little Glass Mountain in foreground; snow-covered Mount Shasta in background. *B*, Southeast lobe of Little Glass Mountain showing continuous surface ridges, many of which are cored by dark coarsely vesicular pumice (CVP).

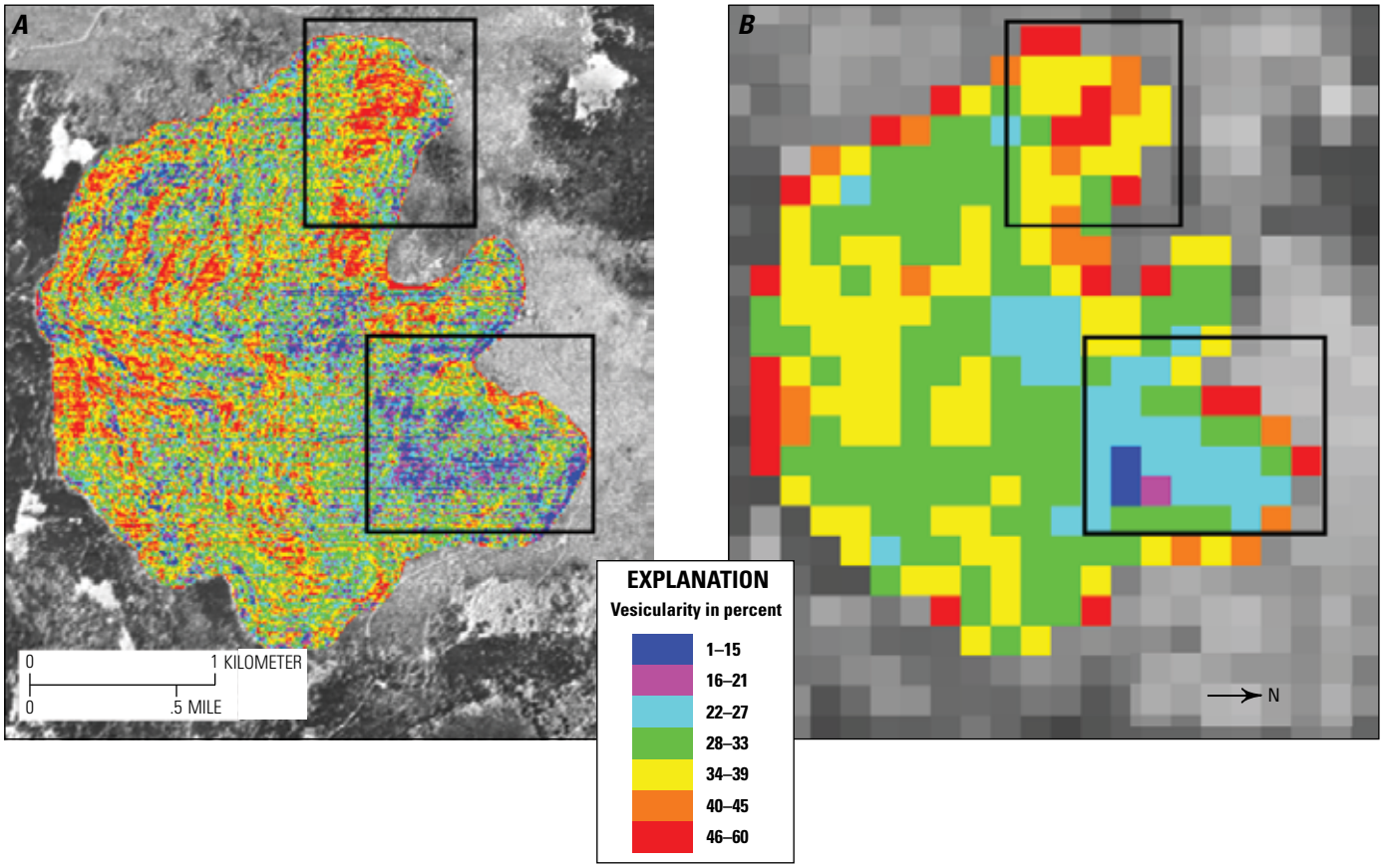

Figure 29. Maps showing thermal infrared spectroscopic maps of emissivity from Little Glass Mountain at two resolutions, corresponding to observations from two different remote-sensing instruments. *A*, Aircraft-based Thermal Infrared Multispectral Scanner (TIMS) image. *B*, Satellite-based Advanced Spaceborne Thermal Emission and Reflection (ASTER) image. Colors correspond to three vesicular textures: 0–27, obsidian (OBS); 28–39, finely vesicular pumice (FVP), and 40–60, coarsely vesicular pumice (CVP). North is to right of photograph. Modified from Ramsey and Fink, 1999.

Scanner (TIMS) airborne instrument (10.4 m/pixel; fig. 29*A*) and the satellite-based Advanced Spaceborne Thermal Emission and Reflection (ASTER) instrument (90 m/pixel; fig. 29*B*). Areas of red and orange correspond to CVP, green and yellow are the more abundant FVP, and blue and magenta indicate OBS and the denser microcrystalline lava found in vent areas.

194.5 Turn right onto U.S. Forest Service Road 43 (USFS 43 N 48). **0.2**

194.7 Turn left onto U.S. Forest Service Road 43A48C. **0.2**

194.9 Park along road. **0.5**

Stop 4. Structural evidence for dikes between and beneath silicic domes

At Newberry and South Sister volcanoes, we observed groups of silicic domes containing structural evidence that suggests they were emplaced by dikes. Medicine Lake also exhibits this geometry, with aligned vents trending northeast on the west side of the volcano and trending northwest on the east side. From Little Mount Hoffman, we could see the main vent at the summit of Little Glass Mountain, as well as the northeast lobe, a distinct flow with its own vent area, which was at least partially erupted prior to the emplacement of the main flow. The N. 30 E.-trending line connecting these two vents continues just west of Little Mount Hoffman and then into the woods for ~3 km before intersecting another group of glass-rich extrusions, the Crater Glass flows (Fink and Pollard, 1983).

The forested zone between the northeast lobe of Little Glass Mountain and the Crater Glass flows contains additional evidence of dike emplacement—an impressive set of ground cracks believed to have formed above one or more laterally flowing or vertically rising rhyolite dikes. When a fluid-filled fracture like a dike rises toward a free surface (that is, the Earth's surface), two parallel zones of tension form, separated by spacing proportional to the depth of the dike top (Pollard and Holzhausen, 1979). Pollard and others (1983) applied this idea to basaltic eruptions in Hawai'i when they observed paired fracture zones

developing above an obliquely rising dike; as the dike approached the surface, spacing between the fracture zones narrowed until the cracks formed a graben from which lava emerged.

Aware of these basaltic studies, Fink and Pollard (1983) proposed that paired sets of ground cracks mapped between Little Glass Mountain and the Crater Glass flows mark the locations of one or more subsurface dikes that likely fed the flows. Ground crack spacings are somewhat challenging to interpret unambiguously, but there are clearly two main groups of cracks separated by about 200 m, suggesting that the dike top is about 100 m below the surface (fig. 30*A*). Crack spacing widens where the cracks go up a prominent hill, implying that the horizontal dike top is further below the Earth's surface under the hill. Further north, the cracks approach the southernmost Crater Glass Flow, and spacing gets smaller as the

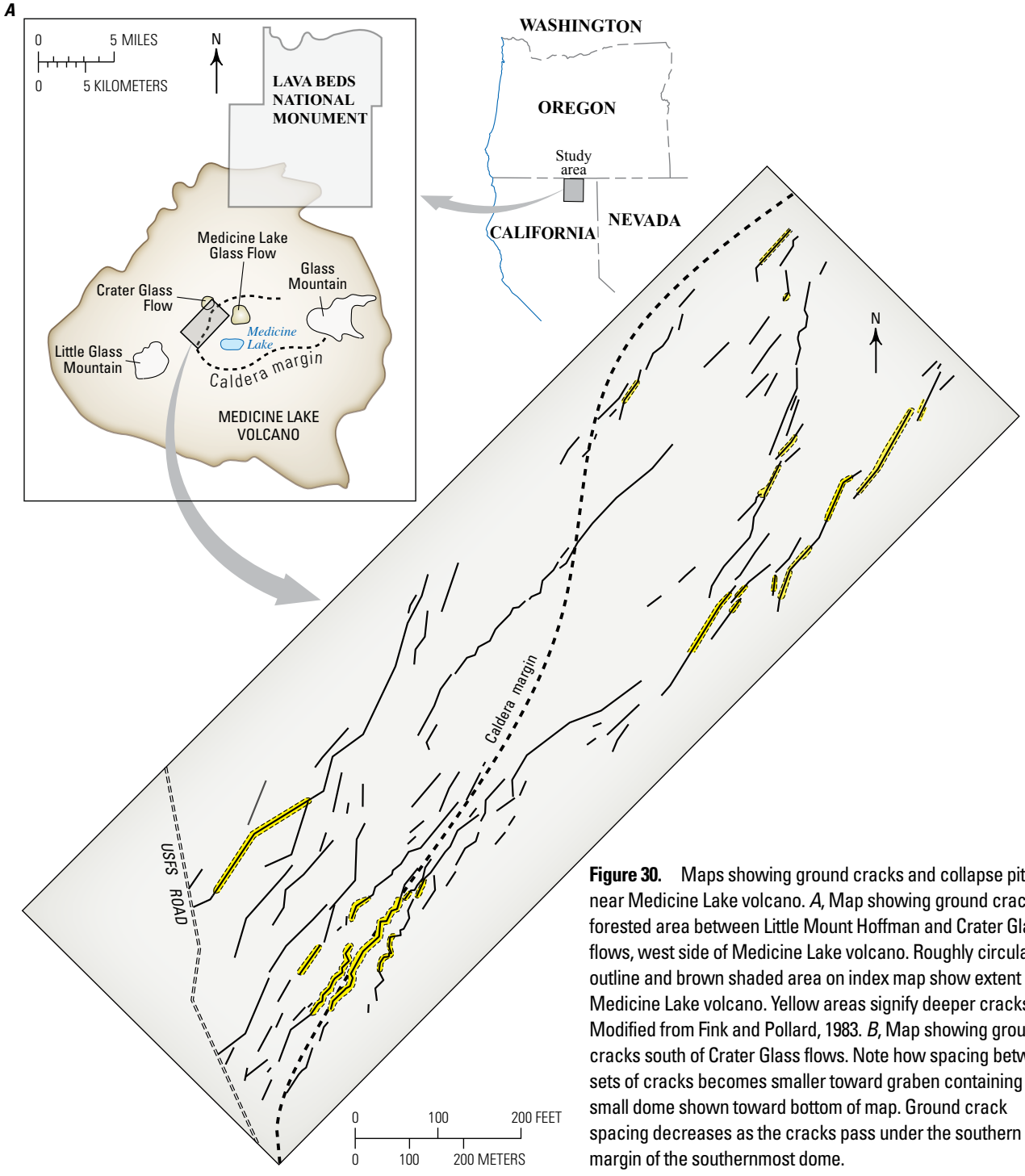

Figure 30. Maps showing ground cracks and collapse pits near Medicine Lake volcano. *A*, Map showing ground cracks in forested area between Little Mount Hoffman and Crater Glass flows, west side of Medicine Lake volcano. Roughly circular outline and brown shaded area on index map show extent of Medicine Lake volcano. Yellow areas signify deeper cracks. Modified from Fink and Pollard, 1983. *B*, Map showing ground cracks south of Crater Glass flows. Note how spacing between sets of cracks becomes smaller toward graben containing small dome shown toward bottom of map. Ground crack spacing decreases as the cracks pass under the southern margin of the southernmost dome.

fracture zone approaches the dome edge (fig. 30*B*). Fink and Pollard (1983) suggested that this decrease in fracture zone spacing near the Crater Glass vent is consistent with the dike top getting closer to the surface, with spacing presumably narrowing in the area buried by the lava flow. About 800 m south of this site, the crack zone contains a small graben composed of three pits, the southernmost of which contains a very small dome. This outcrop might represent an exposure of the dike top, similar to the small domes observed just south of the vent for the Newberry flow on South Sister (fig. 17).

We will spend about an hour walking through this area, tracing the trends of the ground cracks, some of which are as much as 5 m deep (fig. 31). Where the cracks cut through young lava flows, they have very steep walls that trace a zigzag path with strikes that center on the overall N. 30 E. trend (fig. 30*A*). In other places, the cracks run through less competent rock and turn into linear depressions (fig. 30*B*). Even with a theoretical model that appears to explain what was being observed, there can be considerable room for interpretation. We will discuss alternative fracture spacing interpretations while exploring this area.

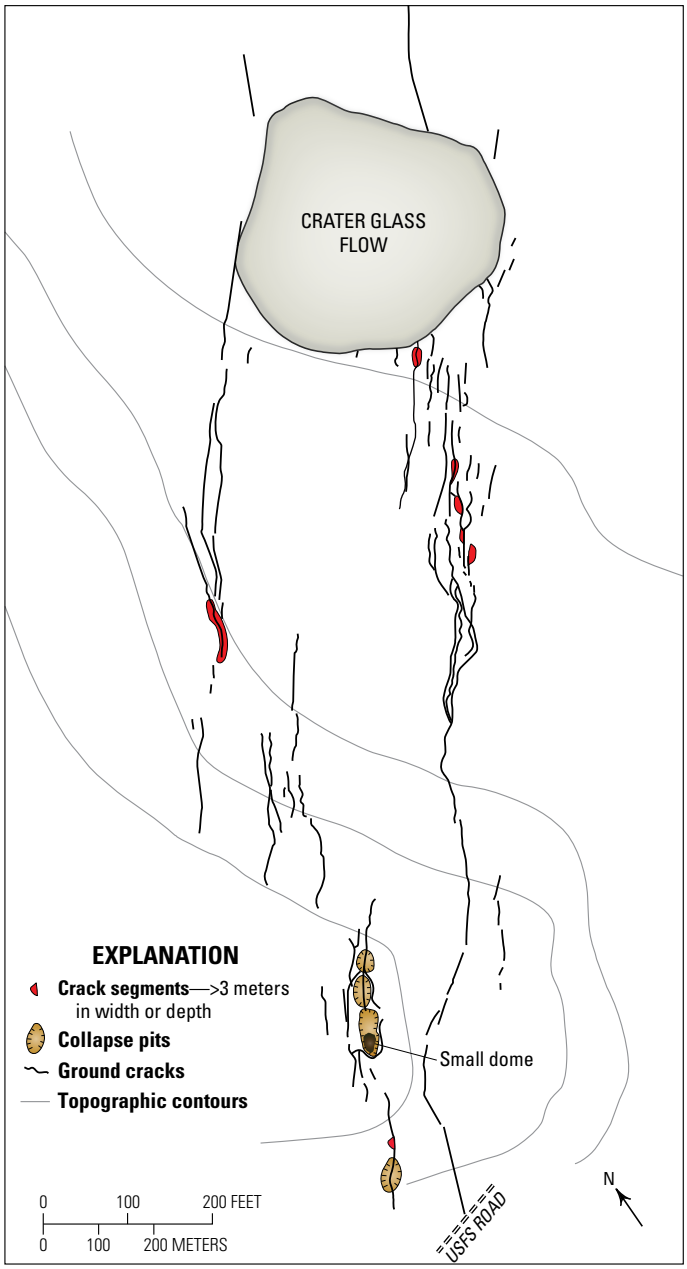

Figure 30.—Continued

Turn around and retrace route back to USFS 43 N 77.

195.4 Turn left to head east on USFS 43 N 77. **2.2**

197.6 Turn right onto Medicine Lake Road. **1.5**

199.1 Turn left onto unmarked road (lat. 41°35′12.41″N., long. 121°35′27.22″W.). **0.3**

199.4 Turn left onto Medicine Lake Road. **0.2**

199.6 Medicine Lake Glass Flow on the left. We will visit this flow tomorrow. **3.0**

202.6 Turn left onto an unmarked road (lat. 41°36′41.24″N., long. 121°37′27.20″W.). **0.3**

202.9 Geothermal workings on the right. **0.2**

203.1 Park along road. We will walk about 1 km southwest along an abandoned road to access the flow front at the intersection of the two largest Crater Glass flows.

Stop 5. Crater Glass flows, dikes and ground cracks

The Crater Glass flows and Little Glass Mountain are thought to be coeval, fed by the same north-northeast-trending dike system that underlies the ground cracks at Stop 4, and made of similar composition lava (silica content of ~71 percent SiO_2; Donnelly-Nolan and others, 2011b, 2016). During this part of the field trip we will explore the largest and smallest of the Crater Glass flows, which preserve morphologic evidence of their dike-fed origin and exhibit exceptionally well-developed, complex CVP crease structures.

Figure 32 shows the route we will take to investigate these domes. From the parking area (1) we will walk 1 km south-southwest along an abandoned road to the front of the two largest, coalesced Crater Glass flows. We will then head to the south end of this pair of domes (2) where prominent ground cracks that emerge from the forest are overridden by lava. Proceeding north again, we will look at a doubly plunging anticline (3) that dips into the flow, cored by CVP and demarcated by outcrops of OBS. This structure

Figure 31. Photographs showing ground cracks near Crater Glass flows. *A*, 4-meter-deep ground crack between Little Glass Mountain and Crater Glass flows. *B*, Depression connected to ground crack, south of southernmost Crater Glass Flow.

Figure 32. Image of Crater Glass flows showing route (dashed white line) and locations (numbered rectangles) for seven stations at Stop 5. Station 1, parking area; station 2, intersection of the dome and prominent ground cracks; station 3, prominent fold visible in flow front; station 4, large smooth area of coarsely vesicular pumice (CVP); station 5, very small dome composed of a single crease structure; station 6, small dome with upper surface dominated by a single fracture; station 7, large explosion crater north of Crater Glass dome trend.

is well exposed in the flow front (fig. 33) and is similar to the one seen earlier on the northwest lobe of Little Glass Mountain (fig. 22). Next, we'll climb up the seam that separates the two largest Crater Glass flows to investigate a broad, roughly circular area of CVP (station 4, fig. 32) cut by a network of curving, en echelon crease structures that have extensive smooth surfaces (fig. 34). As an exercise, we will attempt to reconstruct the sequence through which this part of the flow developed. These two largest Crater Glass flows display an unusually large amount of CVP around their margins, with gently undulating surfaces, relatively small block sizes, and enigmatic, wave-like ridges. In contrast with Little Glass Mountain, the Crater Glass flows lack obvious surface folding, possibly as a result of lower effusion rates (Fink and Griffiths, 1998).

Reversing our route, we will carefully descend the flow and head to the north end of the chain to three outcrops that illustrate stages in the early development of domes that emerge from dikes. Station 5 (fig. 35) looks like a single, asymmetric crease structure with nearly vertical walls. However, this is not a fracture in the surface of a dome—the two walls of the north-northeast-trending structure constitute the entire surface expression of the dome. From here we will climb a short distance onto the next slightly larger dome to the south (station 6, fig. 32). This area (fig. 36) lacks CVP and has a more uniform texture than what we saw on the larger Crater Glass Flow (station 4, fig. 32); its surface is dominated by a medial valley that parallels the crease structure in figure 36 and the overall dome trend. Heading back down this dome, we will walk north to the east side of the northernmost dome in the chain (visible in the background of fig. 35), which is bordered to the north by two colinear, deep explosion craters visible at station 7 (fig. 37), and on its south end by the system of ground cracks that include the very small dome from station 5. The domes shown in figures 35, 36, and 37 can be considered complementary to the very small domes seen the day before on South Sister. Figure 38 shows an interpretation of segmented feeding dike geometry based on evidence on and around the Crater Glass flows.

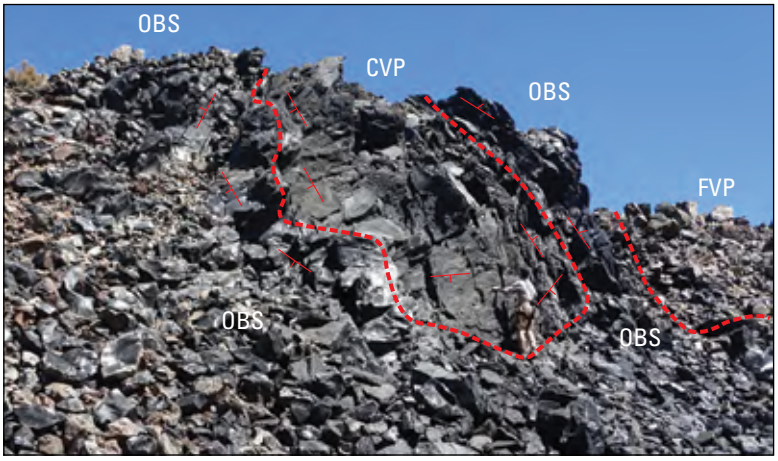

Figure 33. Photograph looking northwest showing doubly plunging anticlinal coarsely vesicular pumice (CVP) outcrop (station 3 in fig. 32) bordered on sides and base by outcrops of obsidian (OBS) with finely vesicular pumice (FVP) visible to the north (right of photo). Dashed red lines separate textural zones. Symbols show representative strikes and dips of flow banding in the lava. Geologist for scale.

Figure 34. Photograph toward southwest showing large relatively smooth area of coarsely vesicular pumice (CVP) (station 4 in fig. 32) on largest of the Crater Glass flows. Note small block size, undulating surface, and cuspate ridges. Distance to prominent tree is approximately 60 meters. Photograph by Hugh Tuffen, professor at Lancaster University.

Figure 35. Photograph looking north along dike trend showing very small dome composed of a single, asymmetric crease structure (station 5 in fig. 32). Northernmost dome of Crater Glass Flow group visible in background.

Figure 36. Photograph looking south along central axis of small dome fed by dike (station 6 in fig. 32). Like shown in figure 35, the entire visible flow represents a fracture surface. Note broad striations on fracture surface to left, around the small tree. Distance to far horizon approximately 100 meters.

Figure 37. Photograph looking south-southwest at pair of craters at north end of Crater Glass Flow alignment (station 7 in fig. 32). Distance to far side of craters is approximately 90 meters.

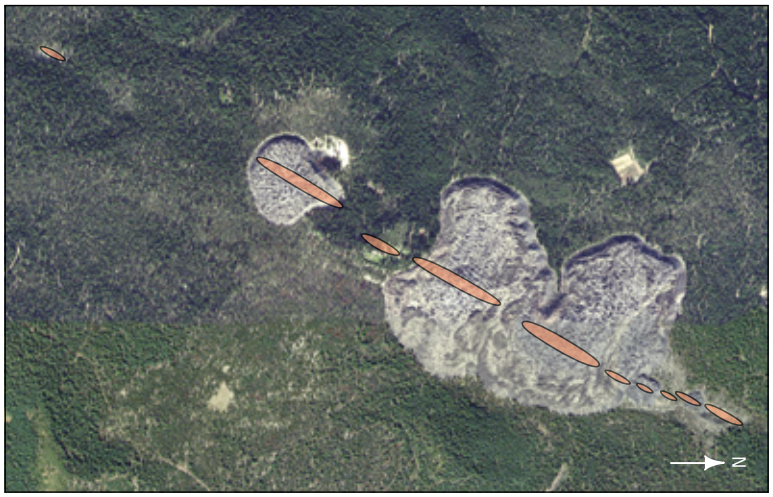

Figure 38. Image showing Crater Glass flows and schematic representation of dike segments believed to have fed the flows.

From here we will walk back east through the woods about 500 m to the parked vans.

203.1 Return on dirt road to Volcanic Legacy Scenic Byway. Turn left. **0.5**

203.6 Head north for to Lava Beds National Monument. **10.7**

214.3 Turn left onto Volcanic Legacy Scenic Byway/ Road 10. **8.4**

222.7 Just past entrance station for Lava Beds National Monument, turn left onto Hill Road/Volcanic Legacy Scenic Byway. **7.7**

230.4 Proceed north to Winema Lodge for the evening.

Day 4—Winema Lodge to East Side of Medicine Lake Volcano to Portland

0.0 Turn right on Hill Road (Volcanic Legacy Scenic Byway). **7.7**

7.7 Turn right onto Road 10/Hill Rd/ Volcanic Legacy Scenic Byway. **2.1**

9.8 Crossing onto Devils Homestead basalt flow. **5.1**

14.9 Schonchin Butte cinder cone on left. The cone erupted ~50,000 years ago (Donnelly-Nolan, 2011b) and emplaced the areally extensive Schonchin Flow that covers most of the monument. The fire lookout post on top of the cone was built between 1939 and 1940 by the Civilian Conservation Corps and is still used today for spotting fires. It was placed on the National Register of Historic Places in 1992. The cone offers excellent views of Lava Beds National Monument, which contains 24 accessible lava tubes and considerable historical information about battles of the Modoc War from 1872 to 1873. **1.2**

16.1 Turn right and head southwest on Volcanic Legacy Scenic Byway/Tennant Lava Beds Road. The road cuts between two older cinder cones, Hippo Butte on the right and Crescent Butte on the left. **2.5**

18.6 Mammoth Crater. Mammoth Crater is the source of much of the basaltic lava that makes up Lava Beds National Monument, including most of the sites of lava tubes (Donnelly-Nolan, 2011b). We will make a quick stop. **8.2**

26.8 Intersection with USFS 44 N 50—continue straight on Volcanic Legacy Scenic Byway. **1.1**

27.9 Medicine Lake Glass Flow on the right. **1.5**

29.4 Turn right onto unmarked dirt trail and park (41°35′36.72″N., 121°35′17.80″W.). **0.3**

Stop 1. Medicine Lake Glass Flow (MLGF)

At this stop, we will climb the flow front of the Medicine Lake Glass Flow (MLGF; also known as Medicine Lake dacite flow, fig. 39) and compare the textural and structural development of this flow surface with that of the glassy rhyolite flows observed previously.

Medicine Lake volcano has erupted at least 9 times during the past ~5 ka, with only Mount St. Helens erupting with a greater frequency in the Cascade Range (Donnelly-Nolan, 2008). The MLGF is part of this

Figure 39. Image of Medicine Lake Glass Flow. Slight color differences represent textural variations on the surface, but are subtler than on the glassy rhyolite flows. Darker areas correspond to crease structures, many of which are aligned in en echelon patterns, particularly in curvilinear bands where the tensional stress field rotated slightly along the trend, similar to the process involved in creating en echelon segments in dikes.

postglacial suite of flows at about 5 ka. The surface is still nearly free of vegetation, except for some areas in the vent area where tephras have accumulated and produced sufficient soil for plants and small trees to grow. Medicine Lake volcano has a summit caldera that formed in response to massive basalt outpourings early in the volcano's history. The MLGF lies entirely within the caldera boundaries. It has a silica content of approximately 68 percent and covers 2.4 km^2 (Donnelly-Nolan and others, 2016). Flow front height ranges from 25 to 40 m, which is generally lower than the height of the rhyolite flows observed the past three days of this field trip.

The textures of this flow have not received the same level of attention as those found on glassy rhyolite flows, but variations do exist. Some areas are dense and glassy with abundant plagioclase phenocrysts, whereas other areas are more vesicular. Some vesicles are pinpoint in size, similar to those seen in FVP areas on glassy rhyolites, whereas others are clearly visible. Because textures are more difficult to discern in the field, they have not been mapped in detail, hampering comparisons between the emplacement histories of this flow and glassy rhyolite flows. Future thermal infrared remote sensing studies might allow for better demarcation of MLGF textures. On the other hand, the structures on this flow have been carefully studied. MLGF displays some of the best examples of crease structures (Anderson and Fink, 1992; figs. 40 and 41).

Observations of several 1980–86 Mount St. Helens dome lobes that were emplaced as single, large crease structures (particularly the October 1980, September 1984, May 1985, and May 1986 dome lobes) provided estimates of strain rate during formation and allowed for modeling of the thermal and mechanical evolution of these structures (Anderson and Fink, 1992). Estimated formation times generated from a one-dimensional conductive cooling model were used to calculate extrusion rates for several older rhyolitic domes emplaced as single crease structures. These emplacement rates varied from less than 1.0 cubic meters per second (m^3/s) for domes in the Devils Hill chain, to more than 100 m^3/s at the Glass Creek dome in the Inyo dome chain (California). These values compare favorably with those determined independently through analysis of overall dome morphology (Anderson and Fink, 1992).

The fracturing process that occurs during crease structure formation is cyclic, with small increments of crack growth alternating with brief periods of cooling. The result is a pair of fracture surfaces lined by striations that parallel the crack axis and form as the crack tip temporarily stops when it hits molten material during

Figure 40. Photograph toward northeast showing crease structure on Medicine Lake Glass Flow. Note presence of progressively smaller blocks outward from central valley, and striations on smooth surface of the crease. These striae represent arrest points during the cyclic fracture formation process, similar to those observed on sides of columnar basalts.

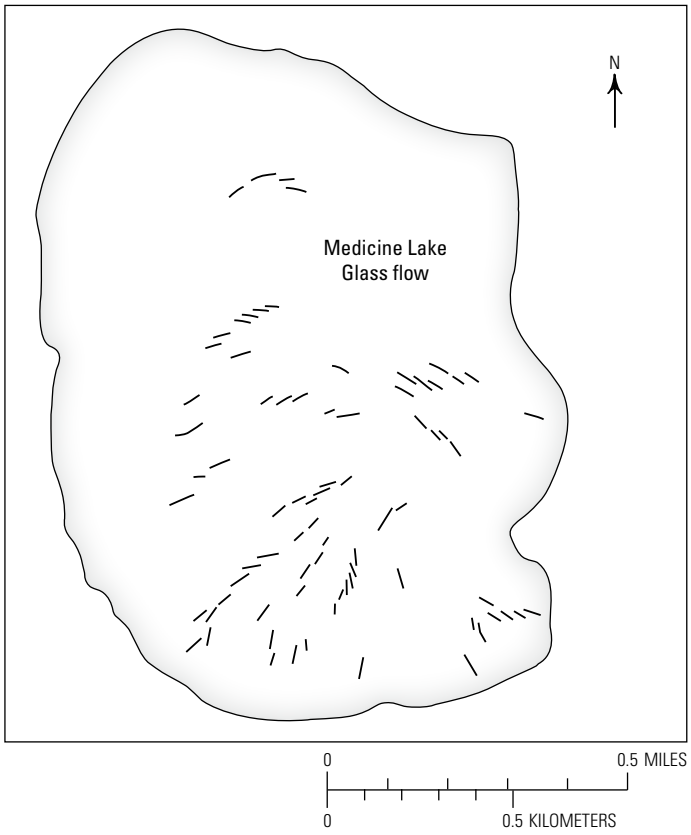

Figure 41. Map showing prominent crease structures on the Medicine Lake Glass Flow from Anderson and Fink (1992). Note en echelon patterns along several of the curvilinear spreading segments.

inward propagation (fig. 42). Similar striae are found on the surfaces of cyclically fractured columnar joints in basalts. On the Medicine Lake Glass Flow many of these striations show vesiculation that occurred during pressure release associated with fracture propagation. This is the only location where this phenomenon has been noted, and it provides some clues about lava rheology during emplacement.

Return to Volcanic Legacy Scenic Byway and turn right.

29.7 Turn left onto U.S. Forest Service Road 44 N 75 (USFS 44 N 75). **1.2**

30.9 Arnica Sink, a flat depression once connected to Medicine Lake, was also a site of considerable geothermal exploration—Turn right at intersection onto USFS 44 N 15. **1.2**

32.1 Intersection of USFS 44 N 15 and U.S. Forest Service Road 97 (USFS 97). Continue straight onto USFS 97. **1.3**

33.4 Turn left onto U.S. Forest Service Road 43 N 99 (USFS 43 N 99). The next 2 km provide views of the Hoffman rhyolite flow on the left. The flow is young (1.2 ka; Donnelly Nolan and others, 2016) but heavily vegetated because of extensive pumice mantling that led to soil formation. **1.7**

35.1 Park along road. **0.0**

Stop 2. Glass Mountain, south side quarry

This stop provides easy access to a pumice mining area known for its textural diversity, and provides some of the best examples of the three primary glassy and vesicular rhyolitic textures found anywhere. Glass Mountain (fig. 43) (also referred to locally as "Big" Glass Mountain) is the largest of a well-studied, voluminous (more than 1.0 km^3), extensive (14 km^2) set of dacite to rhyolite flows (61.3–74.6 percent SiO_2) erupted from as many as 15 distinct vents along a north-northwest-trending fissure on the east side of the volcano (Anderson, 1933; Donnelly-Nolan and others, 2016). The main Glass Mountain eruption began with dacite that transitioned gradually to rhyolite. The lava flows reveal a complex set of mixing relations, which are reflected in the chemistry, petrology, and morphology of individual lobes (fig. 43).

In addition to the range of flow textures found at this site, parts of the flow surface are dotted with explosion pits (fig. 44). These pits formed as volatiles responsible for creating the internal CVP layer reached sufficient pressures to explosively remove OBS and FVP overburden. This process of redistributing volatiles within a flow is responsible for not only the explosion

Figure 42. Photograph showing striae on surface of crease structure on Medicine Lake Glass Flow. Note high degree of vesicularity along individual striations caused by rapid bubble growth in response to pressure release during each cycle of fracture advance. Pen for scale.

Figure 43. Image of Glass Mountain. This large flow ranges from early emplaced dacite that traveled more than 6 kilometers (km) from the vent, to late rhyolite. Dacite-rich areas (labeled on map) appear darker. The prominent rhyolite tongue along the northern boundary of the flow is nearly 2 km long and displays compressional folds further amplified by a gravity instability associated with the rise of coarsely vesicular pumice (CVP). We will park along the southern margin of the flow where mining roads provide easy access to a rhyolitic surface that displays all three texture types, as well as some prominent diapirs of CVP and complexly folded obsidian and pumice layers. Black boxes show areas we will explore at Stops 2 and 3.

Figure 44. Photograph looking northeast showing 5-meter-deep, roughly circular explosion crater in quarry on south side of Glass Mountain. This and other nearby craters are assumed to have formed as volatiles accumulated and exploded from within the internal coarsely vesicular pumice (CVP) layer. Many such pits were destroyed by pumice mining operations.

pits found here, but may lead to the generation of pyroclastic flows from the distal ends of some silicic flows (Fink and Kieffer, 1993).

Also exposed in this quarry is a beautiful assortment of single and multilayer folds composed of alternating bands of pumice and obsidian. Folds have many different scales, with wavelengths and amplitudes that reflect rheologic contrasts between the layers (Castro and Cashman, 1999).

35.1 Continue on USFS 43 N 99. **3.8**

38.9 Turn left on USFS 97. **2.9**

41.8 Continue straight on USFS 43 N 53. **5.4**

47.2 USFS 43 N 53 crosses USFS 97. Bear slightly left to continue on USFS 43 N 53. **1.2**

48.4 Turn left (west) onto USFS 97 (Tionesta Rd). This road is used by large, fast-moving pumice mining trucks. Drive carefully and pull over to the side of the road if a mining truck comes along. At various forks, stay on the better road. You will be driving just north of the early emplaced dacitic lobe of Glass Mountain. **3.8**

52.2 As you enter the pumice mining area, you should see the 75-m-high front of the north lobe of Glass Mountain looming to your left. You will take a sharp left turn onto the access road that goes up onto the lava flow. **0.2**

52.4 Park at the end of the access road that goes up onto the flow. **0.0**

Stop 3. Glass Mountain north lobe

Time permitting, we will stop at the base of the north lobe of Glass Mountain and will walk up the pumice mining road onto the flow surface (fig. 45). This lobe is more than 75 m thick and exhibits textural and structural diversity that is missing in some places as a result of pumice mining operations. Aerial images show that the top of the lobe is covered by regularly spaced ridges interpreted to be compressional folds, with wavelengths proportional to the thickness of the cooled surface crust, and amplitudes enhanced by buoyancy associated with CVP. Each surface ridge is oriented convex downslope. Shear zones along the flow margins cause folds to become greatly attenuated, with pervasive mixing of flow textures in these zones.

From the access road, one can look down on the earlier emplaced dacite lobe, which is darker, thinner, lower, more uniform in texture, and has more scalloped lateral margins. The composition of this dacite lobe gradually becomes more rhyolitic upslope, which can be discerned from the lighter colored FVP in the more silicic parts. The eastern margin of the Glass Mountain flow spills over a steep pre-existing slope, resulting in a few very long narrow lobes and complicated mixing relations chemically and texturally (fig. 43). Detailed mapping of these chemical and textural variations, which would require a combination of remote sensing techniques, could help unravel the fluid dynamic processes that accompanied the emplacement of these enigmatic lavas.

As you hike up the access road, notice the prominent outcrops of aphyric OBS just above you. At about 0.5 miles, the road bends to the right, taking you onto the upper surface where much of the CVP has been extracted by mining; it is difficult to work out the textural relations on this part of the flow. If you have sufficient time, you can hike nearly 2 miles to within 0.5 miles of the Glass Mountain summit. This route shows considerable variation in pumiceous textures and blockiness as it crisscrosses the flow margin shear zones and the folded center of the flow channel. The higher one goes up the flow lobe, the better preserved are the CVP zones.

Retrace route back to the parking area. From here we will drive through Klamath Falls and Eugene to the Oregon Convention Center in Portland. Participants will have Sunday free to explore Portland.

52.4 Drive east down Tionesta Road (USFS 97) to California State Route 139 (CA 139). **13.5**

65.9 Turn left onto CA 139. Follow signs to Tulelake and Klamath Falls. **27.6**

93.5 Cross Oregon border. CA 139 becomes O.R. 39. **17.3**

110.8 Turn left (west) onto O.R. 140. **5.8**

116.6 Head north on U.S. 97 past Chemult, Oregon, to O.R. 58. **82.6**

199.2 Turn left (west) onto O.R. 58 past Oakridge to Interstate 5 (I-5) north just south of Eugene. **85.6**

284.8 Turn north onto I-5 and follow it through Salem to Portland. **100.0**

384.8 At the junction of I-5 and Interstate 205 (I-205), stay on I-5. Proceed through downtown Portland. **14.0**

398.8 Take Exit 302A. Turn right onto NE Weidler. Go 4 blocks to NE Martin Luther King Jr Blvd. **0.2**

399.0 Turn right onto NE Martin Luther King Jr Blvd. **1.6**

400.6 Arrive at Oregon Convention Center. **End of road log.**

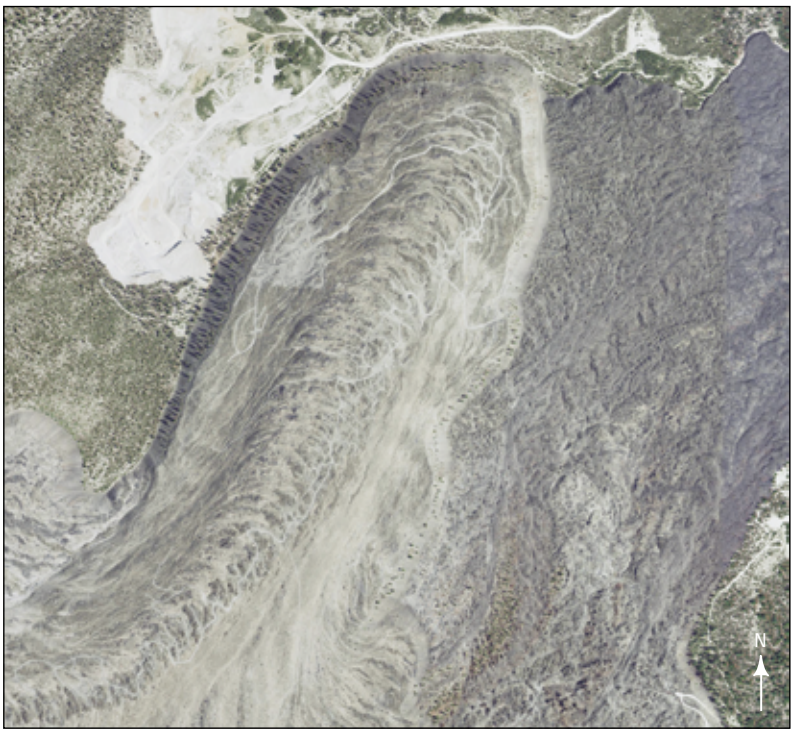

Figure 45. Image showing north lobe of Glass Mountain. Road (white lines) goes up rhyolite lobe, which overrode earlier emplaced dacite lobe. The mining operation preferentially extracted coarsely vesicular pumice (CVP) blocks from surface folds on the north lobe. Note how folds are stretched into finely comminuted shear zones on their east and west ends.

References Cited

Anderson, C.A., 1933, Volcanic history of Glass Mountain, northern California: American Journal of Science 155, p. 485–506.

Anderson, S.W., and Fink, J.H., 1989, Hydrogen-isotope evidence for extrusion mechanisms of the Mount St Helens lava dome: Nature, v. 341, p. 521–523.

Anderson, S.W., and Fink, J.H., 1990, The development and distribution of surface textures at the Mount St. Helens dome, *in* Fink, J.H., ed., Lava flows and domes: Springer Berlin Heidelberg, p. 25–46.

Anderson, S.W., and Fink, J.H., 1992, Crease structures—Indicators of emplacement rates and surface stress regimes of lava flows: Geological Society of America Bulletin 104, v. 5, p. 615–625.

Anderson, S.W., Stofan, E.R., Plaut, J.J., and Crown, D.A., 1998, Block size distributions on silicic lava flow surfaces—Implications for emplacement conditions: Geological Society of America Bulletin 110, v. 10, p. 1258–1267.

Anderson, S.W., McColley, S.M., Fink, J.H., and Hudson, R.K., 2005, The development of fluid instabilities and preferred pathways in lava flow interiors—Insights from analog experiments and fractal analysis, *in* Manga, M., and Ventura, G., eds., Kinematics and Dynamics of Lava Flows: Geological Society of America Special Paper 396, p. 147–161.

Blake, S., and Fink, J.H., 1987, The dynamics of magma withdrawal from a density stratified dyke: Earth and Planetary Science Letters, v. 85, p. 516–524.

Castro, J., and Cashman, K.V., 1999, Constraints on rheology of obsidian lavas based on mesoscopic folds: Journal of Structural Geology, v. 21, p. 807–819.

Castro, J.M., Schipper, C.I., Mueller, S.P., Militzer, A.S., Amigo, A., Parejas, C.S., and Jacob, D., 2013, Storage and eruption of near-liquidus rhyolite magma at Cordón Caulle, Chile: Bulletin of Volcanology, v. 75, no. 4, p. 1–17.

Crandall, D.R., 1989, Gigantic debris avalanche of Pleistocene age from ancestral Mount Shasta volcano, California, and debris-avalanche hazard zonation: U.S. Geological Survey Bulletin 1861, 32 p.

DeGroat-Nelson, P.J., Cameron, B.I., Fink, J.H., and Holloway, J.R., 2001, Hydrogen isotopic analysis of rehydrated silicic lavas—Implications for eruption mechanisms: Earth and Planetary Science Letters, v. 185, p. 331–341.

Delaney, P.T., and Pollard, D.D., 1981, Deformation of host rocks and flow of magma during growth of minette dikes and breccia-bearing intrusions near Ship Rock, New Mexico: U.S. Geological Survey Professional Paper 1202, 61 p.

Donnelly-Nolan, J.M., Grove, T.L., Lanphere, M.A., Champion, D.E., and Ramsey, D.W., 2008, Eruptive history and tectonic setting of Medicine Lake volcano, a large rear-arc volcano in the southern Cascades: Journal of Volcanology and Geothermal Research, v. 177, p. 313–328.

Donnelly-Nolan, J.M, Stovall, W.K., Ramsey, D.W., Ewert, J.W., and Jensen, R.A., 2011a, Newberry Volcano—Central Oregon's Sleeping Giant: U.S. Geological Survey Fact Sheet 2011–3145, 6 p.

Donnelly-Nolan, J.M., 2011b, Geologic map of Medicine Lake volcano, northern California: U.S. Geological Survey Scientific Investigations Map 2927, scale 1:50,000.

Donnelly-Nolan, J.M., Champion, D.E., and Grove, T.L., 2016, Late Holocene volcanism at Medicine Lake volcano, northern California Cascades: U.S. Geological Survey Professional Paper 1822, 59 p., http://dx.doi.org/10.3133/pp1822.

Dzurisin, D., Lisowski, M., Wicks, C.W., Poland, M.P., and Endo, E.T., 2006, Geodetic observations and modeling of magmatic inflation at the Three Sisters volcanic center, central Oregon Cascade Range, USA: Journal of Volcanology and Geothermal Research, v. 150, nos. 1–3, p. 35–54.

Dzurisin, D., Lisowski, M., and Wicks, C.W., 2009, Continuing inflation at Three Sisters volcanic center, central Oregon Cascade Range, USA, from GPS, leveling, and InSAR observations: Bulletin of Volcanology, v. 71, p. 1091–1110.

Eichelberger, J.C., Carrigan, C.R., Westrich, H.R., and Price, R.H., 1986, Non-explosive silicic volcanism: Nature, v. 323, p. 598–602.

Farquharson, J.J., James, M.R., and Tuffen, H., 2015, Examining rhyolite lava flow dynamics through photo-based 3D reconstructions of the 2011–2013 lava flow field at Cordón-Caulle, Chile: Journal of Volcanology and Geothermal Research, v. 304, p. 336–348.

Fink, J.H., 1980a, Surface folding and viscosity of rhyolite flows: Geology, v. 8, p. 250–254.

Fink, J.H., 1980b, Gravity instability in the Holocene Big and Little Glass Mountain rhyolitic obsidian flows, northern California: Tectonophysics, v. 66, p. 147–166.

Fink, J.H., 1983, Structure and emplacement of a rhyolitic obsidian flow—Little Glass Mountain, Medicine Lake Highland, Northern California: Geological Society of America Bulletin 94, p. 362–380.

Fink, J.H., 1985, Geometry of silicic dikes beneath the Inyo Domes, California: Journal of Geophysical Research, v. 90, no. B13, p. 11127–11133.

Fink, J.H., and Anderson, S.W., 2000, Lava domes and coulees, *in* Sigurdsson, H., ed., Encyclopedia of Volcanoes: Academic Press, p. 307–319.

Fink, J.H., and Griffiths, R.W., 1998, Morphology, eruption rates, and rheology of lava domes—Insights from laboratory models: Journal of Geophysical Research, v. 103, p. 527–545.

Fink, J.H., and Kieffer, S.W., 1993, Estimate of pyroclastic flow velocities resulting from explosive decompression of lava domes: Nature, v. 363, no. 6430, p. 612–615.

Fink, J.H., and Manley, C.R., 1987, Origin of pumiceous and glassy textures in rhyolite flows and domes, *in* Fink, J.H., ed., The emplacement of silicic domes and lava flows: Geological Society of America Special Paper 212, p. 77–88.

Fink, J.H., and Pollard, D.D., 1983, Structural evidence for dikes beneath silicic domes, Medicine Lake Highland volcano, California: Geology, v. 11, no. 8, p. 458–461.

Gardner, C., 1994, Temporal, spatial and petrologic variations of lava flows from the Mount Bachelor volcanic chain, central Oregon High Cascades: U.S. Geological Survey Open-File Report 94–261, 100 p.

Gardner, C.A., Scott, W.E., Major, J.J., and Pierson, T.C., 2000, Mount Hood—History and hazards of Oregon's most recently active volcano: U.S. Geological Survey Fact Sheet 060–00, 4 p.

Gardner, J.E., Carey, S., and Sigurdsson, H., 1998, Plinian eruptions at Glacier Peak and Newberry volcanoes, United States—Implications for volcanic hazards in the Cascade Range: Geological Society of America Bulletin 110, p. 173–187.

Hon, K., Kauahikaua, J., Denlinger, R., and Mackay, K., 1994, Emplacement and inflation of pahoehoe sheet flows—Observations and measurements of active lava flows on Kilauea volcano, Hawaii: Geological Society of America Bulletin 106, p. 351–370.

Huppert, H.E., Shepherd, J.B., Sigurdsson, R., and Sparks, R.S.J., 1982, On lava dome growth, with application to the 1979 lava extrusion of the Soufrière of St. Vincent: Journal of Volcanology and Geothermal Research, v. 14, p. 199–222.

Lescinsky, D.T., and Fink, J.H., 2000, Lava and ice interaction at stratovolcanoes—Use of characteristic features to determine past glacial extents and future volcanic hazards: Journal of Geophysical Research, v. 105, no. B10, p. 23711–23726.

Lipman, P.W., 1968, Geology of the Summer Coon volcanic center, eastern San Juan Mountains, Colorado: Colorado School Mines Quarterly, v. 63, no. 3, p. 211–236.

Manley, C.R., and Fink, J.H., 1987, Internal textures of rhyolite flows as revealed by research drilling: Geology, v. 15, p. 549–552.

MacLeod, N.S., Sherrod, D.R., Chitwood, L.A., and McKee, E.H., 1981, Roadlog for Newberry Volcano, Oregon, *in* Johnston, D.A., and Donnelly-Nolan, J., eds., Guides to some Volcanic Terrains in Washington, Idaho, Oregon, and Northern California: U.S. Geological Survey Circular 838, p. 85–91.

Miller, C.D., 1980, Potential hazards from future eruptions in the vicinity of Mount Shasta volcano, northern California. U.S. Geological Survey Bulletin 1503, 43 p.

Nakada, S., Shimizu, H., and Ohta, K., 1999, Overview of the 1990–1995 eruption at Unzen volcano: Journal of Volcanology and Geothermal Research, v. 89, p. 1–22.

Pallister, J.S., Diefenbach, A., Burton, W., Muñoz, J., Griswold, J., Lara, L., and Lowenstern, J., 2013, The Chaitén rhyolite lava dome—Eruption sequence, lava dome volumes, rapid effusion rates and source of the rhyolite magma: Andean Geology, v. 40, no. 2, p. 277–294.

Poland, M.P., Fink, J.H., and Tauxe, L., 2004, Patterns of magma flow in segmented silicic dikes at Summer Coon volcano, Colorado—AMS and thin section analysis: Earth and Planetary Science Letters, v. 219, no. 1, p. 155–169.

Poland, M.P., Moats, W.P., and Fink, J.H., 2008, A model for radial dike emplacement in composite cones based on observations from Summer Coon volcano, Colorado, USA: Bulletin of Volcanology, v. 70, no. 7, p. 861–875.

Pollard, D.D., Delaney, P.T., Duffield, W.A., Endo, E.T., and Okamura, A.T., 1983, Surface deformation in volcanic rift zones: Tectonophysics, v. 94, p. 541–584.

Pollard, D.D., and Holzhausen, G., 1979, On the mechanical interaction between a fluid-filled fracture and the earth's surface: Tectonophysics, v. 53, p. 27–57.

Ramsey, M.R., and Fink, J.H., 1999, Estimating silicic lava vesicularity with thermal remote sensing—A new technique for volcanic mapping and monitoring: Bulletin of Volcanology, v. 61, p. 32–29.

Reches, Z., and Fink, J.H., 1988, The mechanism of intrusion of the Inyo dike, Long Valley Caldera, California: Journal of Geophysical Research, v. 93, no. B5, p. 4321–4334.

Roobol, M.J., and Smith, A.L., 1975, A comparison of the recent eruptions of Mt. Pelée, Martinique and Soufrière, St. Vincent: Bulletin of Volcanology, v. 39, p. 214–240.

Rose, W.I., 1987, Volcanic activity at Santiaguito volcano, 1976–1984: Geological Society of America Special Paper 212, p. 17–28.

Scott, W.E., 1987, Holocene rhyodacitic eruptions on the flanks of South Sister volcano, Oregon, *in* Fink, J.H., ed., The emplacement of silicic domes and lava flows: Geological Society of America Special Paper 212, p. 35–53.

Scott, W.E., and Gardner, C., 1990, Field Trip Guide to the Central Oregon High Cascades, Part I—Mount Bachelor-South Sister Area: Oregon Geology, v. 52, p. 99–117.

Swanson, D.A., and Holcomb, R.T., 1990, Regularities in growth of the Mount St. Helens dacite dome, 1980–1986, *in* Fink, J.H., ed., Lava flows and domes: Springer Berlin Heidelberg, p. 3–24.

Tuffen, H., James, M.R., Castro, J.M., and Schipper, C.I., 2013, Exceptional mobility of an advancing rhyolitic obsidian flow at Cordón Caulle volcano in Chile: Nature Communications, v. 4, no. 2709, 7 p.

UNESCO, 2016, UNESCO Global Geoparks—Celebrating Earth heritage, sustaining local communities: Paris, United Nations Educational, Scientific and Cultural Organization, 20 p., accessed July 2016 at http://unesdoc.unesco.org/images/0024/002436/243650e.pdf.

Watts, R.B., Herd, R.A., Sparks, R.S.J., and Young, S.R., 2002, Growth patterns and emplacement of the andesitic lava dome at Soufriere Hills volcano, Montserrat: Geological Society, London, Memoirs, v. 21, no. 1, p. 115–152.

Wicks, C.W. Jr., Dzurisin, D., Ingebritsen, S., Thatcher, W., Lu, Z., and Iverson, J., 2002, Magmatic activity beneath the quiescent Three Sisters volcanic center, central Oregon Cascade Range, USA: Geophysical Research Letters, v. 29, no. 7, p. 26-1–26-4.

Menlo Park Publishing Service Center, California
Manuscript approved June 2, 2017
Edited by Sarah E. Nagorsen
Design and layout by Cory D. Hurd

ISSN 2328-0328 (online)
https://doi.org/10.3133/sir20175022I